AD-A035 291 AIR FORCE INST OF TECH WRIGHT-PATTERSON AFB OHIO SCH--ETC F/G 20/5
AN ANALYSIS OF MODULATION TECHNIQUES FOR THE SIMULTANEOUS MEASU--ETC(U)
DEC 76 R C CHAPURAN

UNCLASSIFIED GE/EE/76-18 NL

1 OF 2
AD A035291

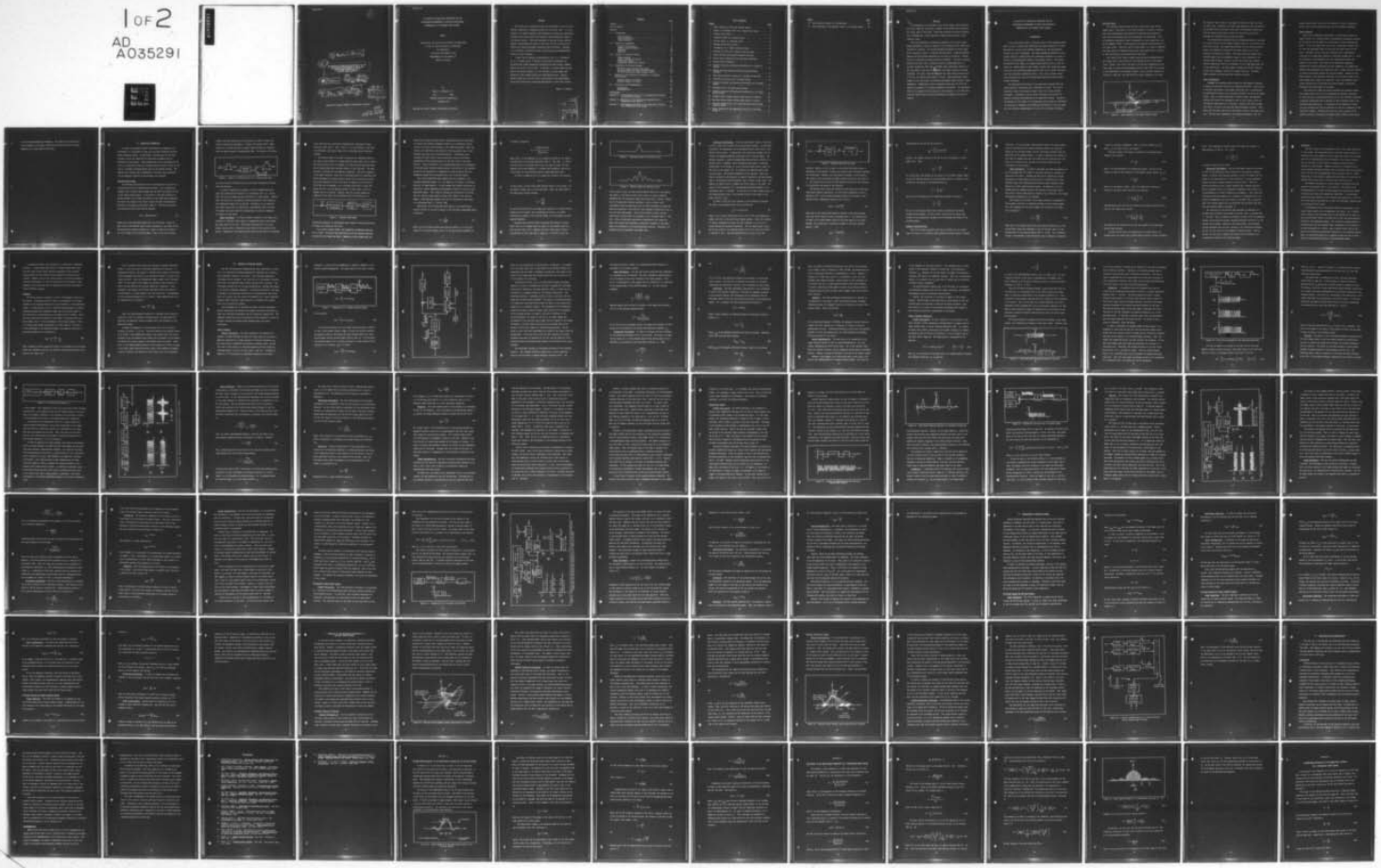

GE/EE/76-18

(1)

(9) Master's thesis,

(6) AN ANALYSIS OF MODULATION TECHNIQUES FOR THE SIMULTANEOUS MEASUREMENT OF RANGE AND REFLECTANCE INFORMATION BY AN AIRBORNE LASER SCANNER •

THESIS

(14) GE/EE/76-18

(10) Charles Robert Chapuran
Capt USAF

(11) Dec 76

(12) 99p.

Approved for public release; distribution unlimited.

GE/EE/76-18

AN ANALYSIS OF MODULATION TECHNIQUES FOR THE SIMULTANEOUS MEASUREMENT OF RANGE AND REFLECTANCE INFORMATION BY AN AIRBORNE LASER SCANNER

THESIS

Presented to the Faculty of the School of Engineering

of the Air Force Institute of Technology

Air University

in Partial Fulfillment of the

Requirements for the Degree of

Master of Science

by

Robert C. Chapuran, B.S.

Capt USAF

Graduate Electrical Engineering

December 1976

Preface

This thesis was accomplished under the sponsorship of the Air Force Avionics Laboratory at Wright-Patterson Air Force Base, Ohio. It is in support of a current program at the laboratory to develop an operational airborne laser scanner which will provide a three-dimensional image of the scanned terrain. This study attempts to describe several possible methods of modulating the output of the laser in such a system and to analyze the system performance resulting from each method. Although it is basically a theoretical study, several practical implementation issues are also discussed.

I would like to express my appreciation to Mr. W. C. Schoonover, Dr. B. L. Sowers and Mr. W. Harmon of the Avionics Laboratory for providing both needed background information and many helpful comments during the course of this study. In addition, a sincere thank you also goes to my faculty advisor, Lt S. R. Robinson, for the support and guidance he has provided during this eight-month period. Finally, special thanks go to my wife, Nita, whose patience and understanding during this period have contributed immeasurably to this final product.

Robert C. Chapuran

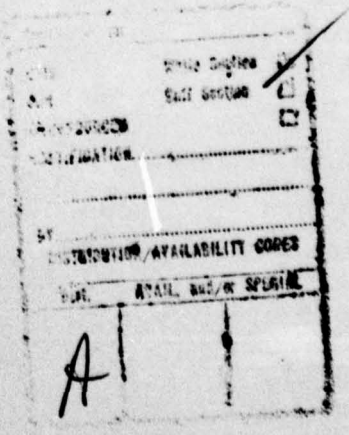

Contents

List of Figures

Abstract

The performance of an airborne laser terrain mapper, which measures both slant range and reflectance, depends on the method used to modulate the output power of the laser. This study analyzes four possible modulation techniques for a direct-detection scanner which utilizes a semiconductor laser.

The first technique is sinusoidal modulation of the laser output. Range performance is found to improve as the frequency of the modulating sinusoid is increased. The second technique modulates the laser output with a subcarrier which is a periodic FM chirp pulse. Range performance improves as the frequency deviation of the chirp is increased. However, this also increases the required detector bandwidth. The third technique modulates the laser with a subcarrier which is phase-modulated by a periodic pseudonoise (PN) code. Although range performance improves as the chip width of the code is decreased, this again requires increased bandwidth. The final technique modulates the laser output directly with a PN code, the output being either on or off. Range performance again depends on the chip width, and improved performance again requires larger bandwidths. Comparisons of these techniques shows that the PN on-off method is preferred if sufficient bandwidth is available. Two configurations for a multiple-source scanner are also proposed. It is shown that both the sinusoid and the PN on-off methods are compatible with such a scanner.

AN ANALYSIS OF MODULATION TECHNIQUES FOR THE SIMULTANEOUS MEASUREMENT OF RANGE AND REFLECTANCE INFORMATION BY AN AIRBORNE LASER SCANNER

I. Introduction

In the past several years, an airborne laser terrain mapping system which is able to obtain both reflectance and range information has been developed for the Air Force Avionics Laboratory by the Environmental Research Institute of Michigan. The range information obtained by this scanner system is combined with the reflectance information in order to provide a three-dimensional image of the scanned surface. With proper processing of this image, the scanner system would be able to pick out objects or targets based on their height profiles even though they might blend into the surrounding background and thus not be readily observable from the reflectance information alone. Thus, such a scanner system could conceivably be used in reconnaissance applications which employ cueing techniques.

The usefulness and accuracy of the range data obtained from this system depend on the method used to modulate the laser. The type of modulation used in the present system is only one of many possible techniques. Furthermore, future system constraints may prevent the present technique from being used in an operational system. Therefore, the purpose of this thesis is to investigate other methods of modulating the laser and to determine the estimation performance of both the range and the reflectance measurements for each of the proposed techniques.

Existing System

The existing scanner system utilizes a mode-locked laser as the signal source. The output of the laser consists of a series of pulses, each pulse approximately one nanosecond in duration and separated in time from the preceding pulse by approximately ten nanoseconds. This ten nanosecond separation, which corresponds to a pulse repetition rate of 100 Megahertz (MHz), is determined by the physical characteristics of the laser cavity. Since the laser is mode-locked, it is able to generate very high levels of transmitted peak power, much higher than it could if it were operating in the continuous-wave (CW) mode.

The output of the laser is swept along the ground perpendicular to the flight path of the aircraft by the rotating action of the scanner (Fig 1, below). The size of the spot on the ground illuminated by this laser beam is called the instantaneous field of view (IFOV) and is equal to one milliradian in the present system. For an aircraft flying at an altitude of 800 feet, the IFOV would thus have a diameter of 0.8 feet.

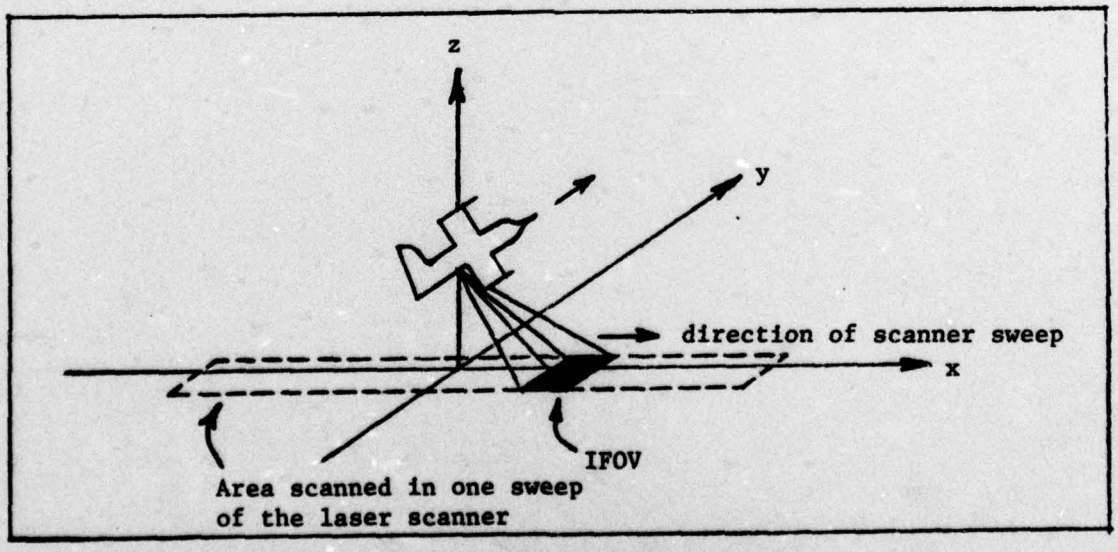

Figure 1. Basic Geometry of the Laser Scanner System

The length of time a point on the ground is within the IFOV is called the dwell time. Obviously, this dwell time depends on both the speed of the aircraft and its altitude, since these two parameters dictate how fast the scanner must rotate in order to cover the entire area by sweeping out contiguous strips along the ground.

The backscattered radiation from the illuminated ground is detected by a power detector in the scanner receiver, where it is converted to an electrical current. The remaining electronics in the receiver detects either the fundamental frequency of the pulse train or one of the harmonics and measures its phase. The phase difference between this received signal and the transmitted signal is then converted to the desired range estimate. However, as with any system that utilizes periodic modulation, there is an ambiguity in the range measurement due to this periodicity. For this system, tracking the 100 MHz frequency results in an ambiguity interval of roughly five feet. Tracking a higher harmonic would decrease this interval even more.

Future Constraints

Although the existing system is ideal for developmental purposes, it may not be practical for use in an operational system. Factors such as the size and weight of the present laser have led to consideration of semiconductor lasers, such as gallium arsenide, for use as the signal source. Also, no matter which type of laser is used, the ambiguity interval will have to be increased so that it is at least as long as the highest target which is of interest. Finally, the scanner system will have to be able to be used with high performance aircraft. This means that the dwell time will be much shorter than in the present system. This may mean, depending on the desired performance, that the

scanner system itself will have to be modified so that it consists of several laser sources instead of just one, as presently configured.

Thesis Overview

Due to the consideration being given to semiconductor lasers as signal sources for a scanner system, the modulation techniques discussed in this thesis will be based on a system which utilizes semiconductor laser. It will be assumed that this laser is peak-power limited; that is, that the peak-power output of the laser can never exceed its CW value. Although a recent study has indicated that a semiconductor laser may not be peak-power limited as previously thought (Ref 1: 6-14), the validity of this assumption will not significantly affect the results of this study. Since each of the modulation techniques analyzed are affected identically by this assumption, the comparisons between these techniques will remain the same. A power detector receiver, as used in the present system, will also be assumed. Because of this power detector, only amplitude variations in the received power of the laser signal will be able to be detected. Thus, the modulation techniques analyzed will of necessity be various methods of amplitude-modulating the output power of the laser.

This report will begin by briefly reviewing the parameter estimation theory which will be used in analyzing the proposed techniques. It will then give a detailed description of the four different modulation techniques investigated and an analysis of each technique based on the previously-described theory. A discussion of the ambiguity interval for each technique will also be provided, as well as a comparison of the individual methods. Following this will be a brief analysis of two possible methods of setting up a multiple source scanner system, based

on the proposed modulation techniques. The report will conclude with a brief summary of the basic findings of the study and several recommendations for future work in this area.

II. Theoretical Background

In order to accurately analyze the modulation techniques to be considered, it is necessary to make use of several concepts from parameter estimation theory. In particular, the equations for the error variance of both the range and the reflectance estimates will be developed in this chapter. These expressions will be developed for the case of a system which utilizes a matched filter receiver as well as the case of a harmonic tracking system (such as the present system). The chapter will conclude with a discussion of both the range resolution and the ambiguity interval of the systems to be analyzed.

Matched Filter System

The necessary equations will first be developed for the case of a system which utilizes a matched filter receiver. Such receivers are commonly used in modern radar systems and can easily be adapted for use in the laser scanner system. If the output of the power detector is passed through a filter which is matched to the signal which modulates the laser, the output of the filter is just the time autocorrelation function of the signal itself (Fig 2, page 7). This time autocorrelation function can be found from the equation

$$R(\tau) = \int_0^T s(t)s(t+\tau)dt \qquad (1)$$

where s(t) is the modulating signal and T is its period. Thus, the peak value of the matched filter output corresponds to the value of the autocorrelation function evaluated at τ equal to zero and is equal to the total energy in the received signal. Thus, in the laser scanner

system, this peak amplitude can be processed in order to obtain the desired reflectance information. Further, the matched filter output signal can be routed through a threshold detector which is triggered when the signal exceeds a predetermined level. The range to the object

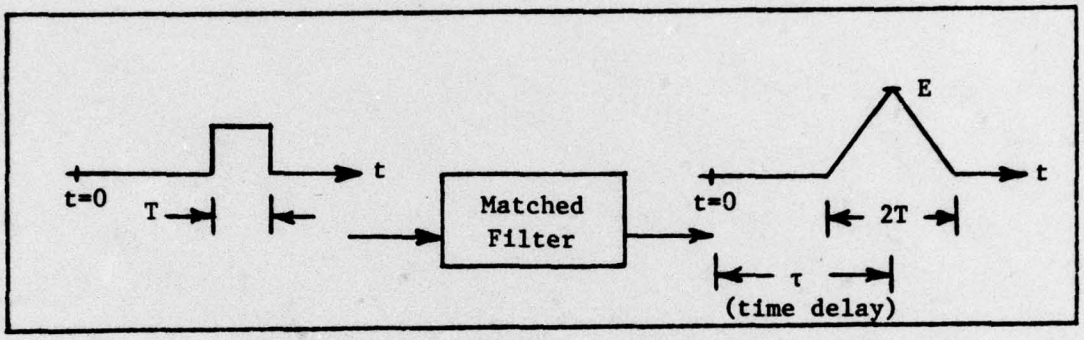

Figure 2. Output of a Matched Filter for a Single Pulse Input

can then be easily calculated from the time delay information obtained from this detector.

In order to simplify the problem, it will be assumed that both range and reflectance are constant in a resolution cell, i.e., in the IFOV, and that the signal has been reflected by a point target. Furthermore, the effects of the spatial filtering operation of the scanner on the transmitted signal will be ignored. Although it is not expected that these effects will be significant, nevertheless, this is an area of further study which should be accomplished in order to complement the results of this study.

Range Performance. In order to obtain a measure of the range error variance of a matched filter system, an expression known as the Cramer-Rao lower bound can be used. This bound, when applied to the laser scanner system, gives a theoretical lower bound on the accuracy of the system. Depending on the signal-to-noise ratio and the type of processing

used, this bound can actually be asymptotically approached in many practical cases (Ref 2: 109). Thus, it is a good measure to use both in evaluating a particular system and in comparing several different systems.

The receiver model to be used in applying the Cramer-Rao bound to the laser scanner system is a simple additive noise model (Fig 3, below). The noise process, n(t), is assumed to be additive white Gaussian noise with a double-sided power spectral density of $N_0/2$ watts/Hz. The power detector is divided into two separate components. The first component is the power converter, which has a conversion factor of R amps/watt and which transforms the received optical power into an electrical current. The second component is the filter which is inherent in the detector. The filter will be assumed to be a low-pass filter with a cutoff frequency of W Hz. For the analysis portion of this study, it will be assumed that W is infinite. However, when the various systems are compared to each other, the filtering action of the detector is a

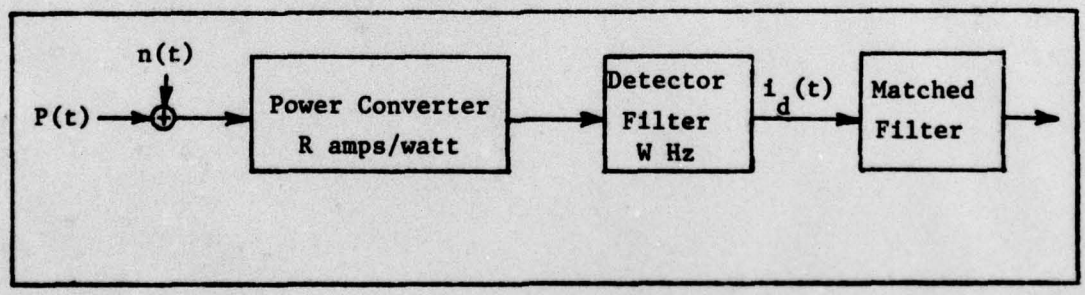

Figure 3. Receiver Noise Model

significant parameter in determining their relative merits and thus will be taken into account at that time.

In an actual scanner system, the assumption of Gaussian noise may not be valid. This would thus invalidate use of the variance equation derived from the Cramer-Rao bound. However, it can be shown that the

range error variance derived using a leading-edge analysis which does not require the Gaussian assumption results in an expression fairly close to the lower bound provided by the Cramer-Rao method. Thus, the results to be derived can be applied to the more general case of non-Gaussian noise with very little modification. This general case includes all other types of noise statistics, such as the Poisson distribution which is characteristic of the shot noise of the power detector. Since the details of the leading-edge analysis are dependent on the particular technique being analyzed, calculation of the variance derived by this method and a comparison of these variances with the Cramer-Rao bounds will be postponed until the following chapter.

Use of the Cramer-Rao bound assumes that the frequency of the received modulating signal, i.e., the signal at the output of the power detector, is known exactly. It also assumes that several conditions of regularity, usually adequately approximated in practice, are met by the modulating signal. And, finally, although the derivation of the bound does not require a high signal-to-noise ratio (SNR) in the received signal, a high SNR (much greater than one) is required for this bound to be approached (Ref 2: 115-119, 300).

Application of the Cramer-Rao lower bound to the matched-filter receiver results in an error variance of the time delay measurement which is given by

$$\sigma_\tau^2 = \frac{N_0}{2E\beta^2} \tag{2}$$

where $N_0/2$ is the double-sided noise spectral density, E is the total energy in the received signal, and β^2 is the mean-squared bandwidth of

the signal, defined as

$$\beta^2 = \frac{4\pi^2 \int_{-\infty}^{\infty} f^2 |U(f)|^2 df}{\int_{-\infty}^{\infty} |U(f)|^2 df} \tag{3}$$

where $|U(f)|$ is the magnitude of the frequency spectrum of the complex representation of the signal modulation (Ref 2: 299, 300). It should be noted that β^2 as defined above is not the same as either the more commonly used noise bandwidth or 3 decibel (db) bandwidth, and must be recalculated for each different type of signal modulation used.

In order to change Eq (2) to a range error variance, the relation

$$2r = c\tau \tag{4}$$

is used, where r is the slant range from the sensor to the target, c is the speed of light, and τ is the time delay. Thus, the lower bound of the range error variance becomes

$$\sigma_r^2 = \frac{c^2 N_0}{8E\beta^2} \tag{5}$$

As can be seen from Eq (5) the range error variance of a matched filter system can be decreased, thus increasing the accuracy, by either increasing the energy of the received signal or by increasing its mean-squared bandwidth.

One more point should be made concerning this measure of range error; that is, it assumes that the output of the matched filter has only one main lobe, and it computes the error bound based on noise perturbations of this lobe (Fig 4, page 11). In reality, since the

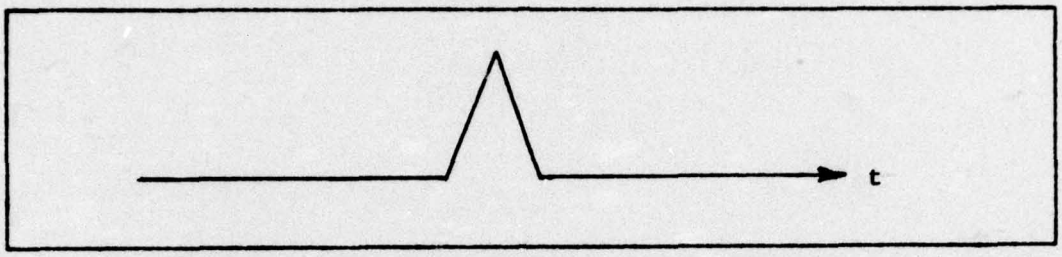

Figure 4. Idealized Output of a Matched Filter

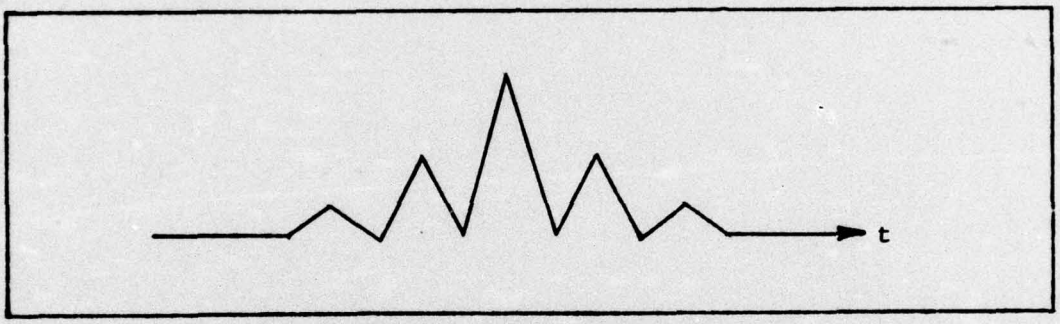

Figure 5. Typical Output of a Matched Filter

filter output is just the time autocorrelation function of the modulating signal, it may have one main lobe as well as several sidelobes depending upon the particular signal being used (Fig 5, above). Depending on the amplitude of these sidelobes, a burst of noise could conceivably cause the amplitude of one of these sidelobes to exceed the detection threshold of the receiver, thus causing an additional error in the time delay measurement. This is the problem of global accuracy versus local accuracy which is discussed in the literature (Ref 3: 294-307). Thus, an additional qualitative consideration that should be taken into account when analyzing a modulation technique is the amplitude of the sidelobes of the autocorrelation function. Obviously, low sidelobes are more desirable than higher ones.

Reflectance Performance. The other performance measure of interest is that of the error variance of the reflectance estimate. As mentioned previously, the reflectance can be estimated from the peak value of the matched filter output. In particular, the reflectance estimate can be obtained by maximum-likelihood processing of the received signal. For analysis purposes, a typical maximum-likelihood processor consists of a matched filter, a sampler, and an attenuator whose gain is inversely proportional to the energy, E, in the received signal (Fig 6, page 13). The noise in the system, n(t), is assumed to be additive white noise with zero mean. The Gaussian assumption is not required. Thus, the results derived by this analysis can again be applied to the more general case of non-Gaussian noise statistics, such as those of shot noise. The sampler is timed so that it samples the filter output at its peak. The output of this processor is $\hat{\rho}$, the maximum-likelihood estimate of the reflectance (Ref 4: 589-590). In the case of the laser scanner receiver, the noise-corrupted input to the matched filter is the output of the power detector, $i_d(t)$.

In order to find the error variance of the reflectance estimate, the input to the matched filter will be written as

$$i_d(t) = \rho s(t) + n(t) \tag{6}$$

where ρ is the actual reflectance value, s(t) is the laser modulating signal, and n(t) is the white-noise random process. Since the processor is linear, superposition holds, and each component of $i_d(t)$ can be traced through the processor separately. For the signal input, $\rho s(t)$, the filter output at the sampling instant will be ρE, since the filter is matched to s(t). After multiplying this by a gain of 1/E, the

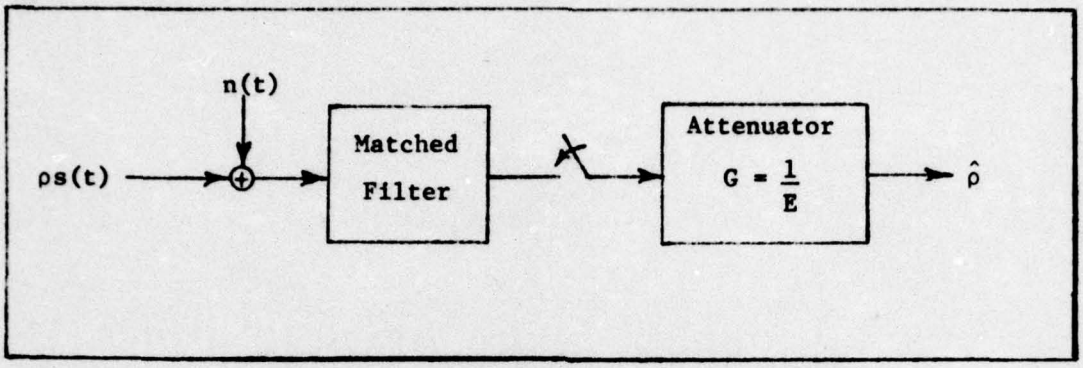

Figure 6. Maximum Likelihood Processor

processor output, $\hat{\rho}$, will be equal to the actual reflectance value, ρ. Therefore, in the absence of noise, the receiver will accurately estimate the reflectance. However, the noise which is present in the receiver will result in the reflectance estimate varying around the true value of ρ. The variance of the error in this estimate will thus be the variance of the noise at the output of the receiver.

The easiest way to find the variance of this noise is by using the known power spectral densitites. If the Fourier transform of s(t) is denoted by S(f), then the power spectral density of the output of the matched filter, assuming an input of n(t), will be

$$S_0(f) = |S(f)|^2 \frac{N_0}{2} \tag{7}$$

where $N_0/2$ is the double-sided spectral density of the noise process. Since the filter output is also a zero-mean process, its variance will be equal to its second moment, which is the noise power at the output. However, this noise power is just the integral of the power spectral density. Thus,

$$\sigma_{MF}^2 = \int_{-\infty}^{\infty} S_0(f)df \tag{8}$$

Substituting Eq (7) into Eq (8) results in

$$\sigma_{MF}^2 = \frac{N_0}{2} \int_{-\infty}^{\infty} |S(f)|^2 df \tag{9}$$

However, the integral portion of Eq (9) is just the energy, E, in the signal s(t). Thus,

$$\sigma_{MF}^2 = \frac{N_0 E}{2} \tag{10}$$

As a final step, the variance of the noise at the receiver output, which is also the desired variance of the reflectance error, is related to the variance at the output of the matched filter by

$$\sigma_{\rho}^2 = \frac{1}{E^2} \sigma_{MF}^2 \tag{11}$$

Thus, the error variance of the reflectance estimate is given by

$$\sigma_{\rho}^2 = \frac{N_0}{2E} \tag{12}$$

Eq (12) is the relation which will be used in analyzing the various matched filter systems. As can be seen, the only way to improve the accuracy of the reflectance estimate is by increasing the energy of the received signal.

Harmonic Tracking System

The error variance equations will next be derived for the second type of systems to be analyzed, those systems utilizing harmonic tracking

receivers. As in the present laser scanner system, the range estimate will be calculated from the phase difference between the reference signal and the received signal, and the reflectance estimate from the amplitude of the received signal. In order to simplify the problem, it will again be assumed that both the range and the reflectance are constant in a resolution cell and that the received signal has been reflected by a point target.

Range Performance. In order to determine the range performance, it will be assumed that the output of the power detector is tracked by a phase-lock loop (PLL). Although the PLL may not improve the system performance at high signal-to-noise ratios, it typically has a lower threshold than other techniques and thus will permit adequate system operation at lower signal-to-noise ratios. In addition it will be assumed that the dominant noise in the receiver is zero-mean, white noise with a double-sided spectral density of $N_0/2$ watts/Hz. Once again, the Gaussian assumption is not required.

The variance of the error in the range estimate is determined by the accuracy of the PLL in tracking the phase of the received signal. For a PLL operating in its linear region, the variance of its phase error is given by

$$\sigma_\phi^2 = \frac{N_0 W_L}{2P_c} \tag{13}$$

where $N_0/2$ is the double-sided noise power spectral density, W_L is the double-sided closed loop bandwidth of the PLL (in Hz), and P_c is the average power in the received signal (Ref 5: 27-30). For a harmonic tracker, the bandwidth of the PLL need be only as large as is required

to pass the spectral information. Thus, W_L will be roughly $2/\tau_d$ Hz, where τ_d is the dwell time of the scanner.

The slant range to the target is related to the measured phase change by the relation

$$2r = \frac{\phi}{2\pi} \lambda \tag{14}$$

where λ is the wavelength of the modulating signal. Eq (14) can be written in terms of the frequency of the harmonic being tracked, f_m, as

$$r = \frac{c}{4\pi f_m} \phi \tag{15}$$

where c is the speed of light. Thus, the range error variance is related to the phase error variance by the relation

$$\sigma_r^2 = \left(\frac{c}{4\pi f_m} \right)^2 \sigma_\phi^2 \tag{16}$$

Substituting Eq (13) into Eq (16) results in the equation which will be used for the range error variance:

$$\sigma_r^2 = \left(\frac{c}{4\pi f_m} \right)^2 \frac{N_0}{P_c \tau_d} \tag{17}$$

The values for the variables in Eq (17) will depend on the particular system being analyzed.

In order for the PLL to be operating in its linear region, as assumed above, the phase error variance must be below a certain threshold

value. This threshold is usually taken to be where the variance is approximately 1/4 (Ref 6: 23). Thus,

$$\sigma_{\phi}^{2} = \frac{N_0}{P_c \tau_d} \leq \frac{1}{4} \tag{18}$$

in order for Eq (17) to be valid.

Reflectance Performance. The last performance measure of interest is that of the reflectance error variance for the harmonic tracking system. To derive this variance equation, it will be assumed that the output of the power detector is first mixed with a locally generated replica and then is passed through a low-pass filter. Thus, the receiver structure is just a Radio Frequency (RF) coherent detector. Since a low-pass filter is an imperfect integrator, this receiver can be approximated by a mixer followed by an integrator. Also, since the reflectance has been assumed to be constant in a resolution cell, the period of integration can be set equal to one dwell time, τ_d seconds. Thus, the received signal will be integrated over one dwell time each time the receiver makes an estimate, $\hat{\rho}$.

The structure of the receiver just described is identical to a matched filter receiver which samples the output every τ_d seconds (Ref 7: 247-249). Thus, by adding an attenuator of gain 1/E to the harmonic system, the receiver has become a maximum-likelihood receiver as in the matched filter system. Because of this equivalence, the previously derived expression for the error variance of the reflectance estimate, Eq (12), is also valid for the harmonic tracking receiver. Also as before, the only way to improve the accuracy of the estimate is by increasing the energy of the received signal.

Resolution

The next concept to be described is that of the range resolution of the system. The range resolution of the laser scanner system is a measure of how close together in slant range two objects can be placed and still be distinguished from one another by the scanner receiver. This is equivalent to the concept of nominal resolution which is defined for radar systems. Nominal resolution is a measure of how close together individual targets, such as aircraft flying in formation, can be and still be distinguishable from one another (Ref 8: 88-93). Resolution, as thus defined, ignores both the effects of noise and all spatial effects and, thus, is the best that a system can do.

The nominal resolution of a radar system is determined from the output of the matched filter in the receiver. Two targets can be distinguished only if their returned signals are separated far enough in time so that they can be separately identified. A conventional, though arbitrary, measure of this required time separation is that the two returns must be separated by at least the half-power response width of the matched filter output.

The extension of this conventional measure of resolution to the laser scanner system can be accomplished very easily. For a matched filter receiver, the half-power width of the matched filter output is just the half-power width of the main lobe of the time autocorrelation function of the modulating signal. For a harmonic tracking receiver, the phase-lock loop and low-pass filter combination can be thought of as being equivalent to or better than a matched filter just as was done in the reflectance performance derivation in the preceding section. Thus, the resolution measure for a harmonic system can also be found from the autocorrelation function of the modulating signal.

As mentioned earlier, this definition of resolution is completely arbitrary. A given system may be able to resolve ranges much closer than the above criteria would indicate, depending on such receiver characteristics as the setting of the threshold in a matched filter receiver. However, even if the criteria gives a worst-case estimate of resolution performance, it still is useful both for obtaining a rough estimate of the resolution and for comparing the relative advantage of several different systems.

Ambiguity

The final concept of interest is that of the ambiguity interval of the system. As mentioned earlier, there is an ambiguity in the range estimate of the existing system due to the periodicity of the modulating signal. In this system, as in any harmonic tracking system, the phase difference between the transmitted signal and the received signal is not unique due to the periodicity of the phase every 2π radians. Since the slant range from the scanner to the target is calculated from the phase change, there is also an ambiguity in the range estimate. Since a 2π radian phase change corresponds to a slant range of $\lambda/2$, where λ is the wavelength of the modulating signal, the ambiguity interval of the range estimate can be expressed as

$$r_{amb} = \frac{\lambda}{2} = \frac{cT}{2} = \frac{c}{2f_m} \tag{19}$$

Thus, although the slant range may be able to be estimated very accurately within this ambiguity interval, the receiver cannot determine which $(\lambda/2)$ interval the range is in.

Since a matched filter system also utilizes a periodic modulating signal, it will also have an associated range ambiguity interval. As explained previously, the range in a matched filter system is calculated from the measured time delay for the transmitted signal to travel to the target and back. Since the transmitted signal repeats every T seconds, where T is the period of the signal, the receiver cannot determine in which T-second interval the received signal was transmitted. Thus, although it can measure the relative time delay within the current T-second interval, it cannot measure the total time delay. Corresponding to this time-delay ambiguity is, of course, a range ambiguity which can be represented by the equation

$$r_{amb} = \frac{cT}{2} = \frac{c}{2f_m} \tag{19}$$

Thus, the range ambiguity interval for a matched filter system is identical to that of a harmonic tracking system. As might have been expected, the ambiguity interval depends only on the frequency of the modulating signal.

Although the ambiguity of the system may seem to be a serious problem, in reality, it is not. Since the purpose of the scanner system is to obtain a three-dimensional image of the scanned area, the item of interest is not the absolute slant range from the scanner to the targets, but rather the relative ranges of the targets with one another. Therefore, if the range ambiguity interval of the system is at least as large as the slant range differential which results from scanning the highest target of interest, the operation of the scanner will not be degraded.

III. Analysis of Proposed Systems

Now that the theoretical background has been established, the next step is to describe the proposed modulation techniques and to analyze each technique by means of this theory. Four different modulation techniques will be analyzed. The first one is of the harmonic tracking type, while the remaining three utilize matched filter receivers. The techniques analyzed are not the only possibilities, although they appear to be the most promising techniques. As mentioned previously, the laser is assumed to be peak-power limited with a continuous-wave (CW) output power of P_a watts, and the receiver is assumed to be a direct detection receiver, which utilizes a power detector to transform the received power into an electrical current.

Each technique will be described in detail by first providing a general description and system block diagram, and then by deriving its range and reflectance performance and its resolution capabilities. The ambiguity problem will also be discussed for each technique, as well as possible problems concerning system implementation and overall feasibility.

Single Sinusoid

General Description. The first technique to be analyzed is a harmonic tracking technique in which the output power of the laser is amplitude modulated by a single sinusoid of arbitrary frequency, f_m. The laser output is generated very simply by adding a direct current (DC) bias to the output of a sine-wave generator and then using the resulting signal to excite the laser (Fig 7, page 22). Although the addition of a DC bias may be accomplished internally by the laser

modulator, it will still be considered as a separate component of the overall system configuration. The output power of the laser is given

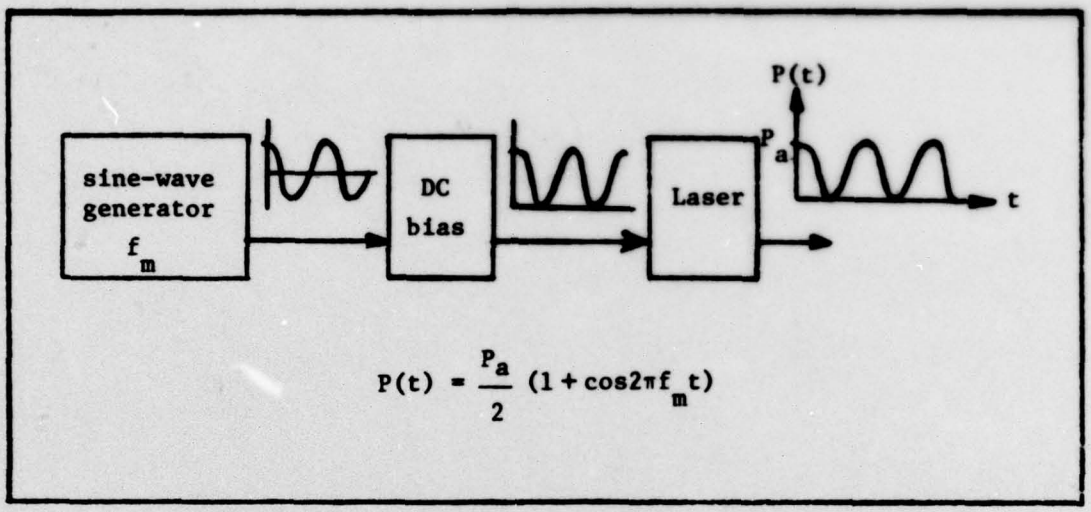

Figure 7. Transmitter for a Single Sinusoid System

by the equation

$$P(t) = \frac{P_a}{2}(1+\cos 2\pi f_m t) \tag{20}$$

The receiver structure for this single sinusoid system is similar to that of the present system in that it tracks the received sinusoid and measures range by calculating the phase change between the transmitted signal and the received signal (Fig 8, page 23). In particular, the received signal, P(t), is first detected by a power detector which converts it to a current, $i_d(t)$, of value

$$i_d(t) = \frac{P_a R}{2}(1+\cos 2\pi f_m t) \tag{21}$$

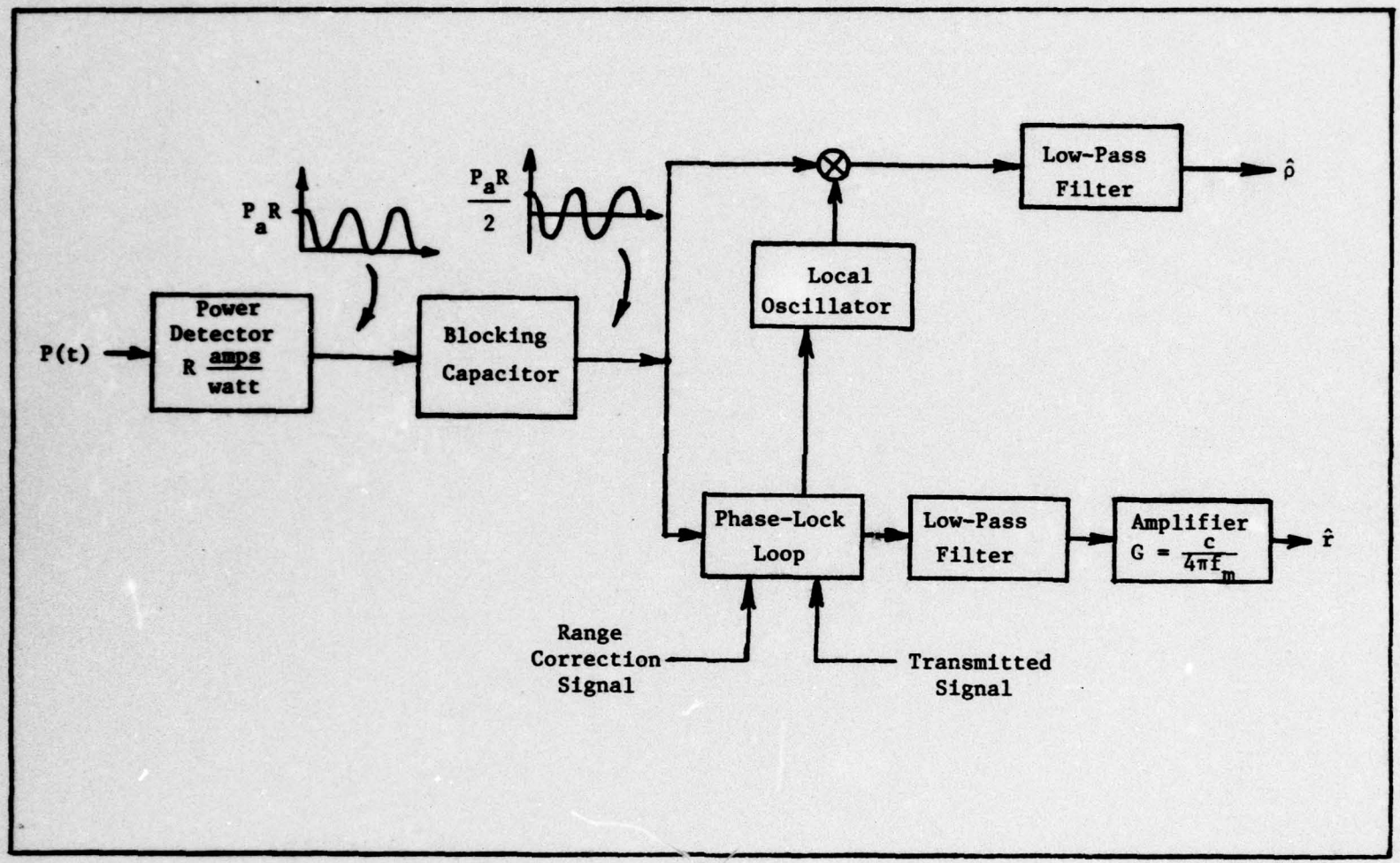

Figure 8. Receiver Structure for a Single Sinusoid System

where R is the responsivity of the detector, in amps/watt. For simplicity, the power losses due to such things as the distance between the transmitter and the target, atmospheric attenuation, and losses in the optics of the system have been ignored since they are the same for all of the systems to be discussed.

The detector current, $i_d(t)$, is then passed through a blocking capacitor in order to eliminate the DC term. Although this filtering action may be inherent in the power detector itself, it again will be considered as a separate element in the system configuration. The resulting sinusoid, of amplitude $P_a R/2$, is used to calculate both the range and the reflectance estimates. The range is calculated by means of a phase-lock loop (PLL) which tracks the phase of the sinusoid and compares it to a reference signal. By providing both the transmitted signal and a range correction signal, which corrects for the geometry of the scanning process, as inputs to the PLL in addition to the received sinusoid, the output of the PLL is the phase change that corresponds to the corrected slant range from the scanner to the target. If desired, a further range correction can be included which would subtract off the slant range to a horizontal ground plane. The PLL output in this case would approximate the height of the target above the ground plane. A low pass filter after the PLL eliminates the double frequency term which is generated by the PLL, and the amplifier which follows converts the measured phase change into the desired slant range estimate.

The reflectance estimate is calculated by means of an RF coherent detector. The incoming sinusoid is mixed with a locally generated replica, and the result is passed through a low-pass filter. The

resulting reflectance estimate is a maximum-likelihood estimate, as explained in the previous chapter.

Range Performance. Now that the overall system has been explained, its performance can be analyzed. The first performance characteristic to be considered is the error variance of the range estimate. Since Eq (17) is applicable to this system, the only variable to be calculated is the average power in the received signal, P_c. For the received sinusoid,

$$P_c = \frac{\left(\frac{P_a R}{2}\right)^2}{2} = \frac{P_a^2 R^2}{8} \tag{22}$$

Substituting Eq (22) into Eq (17) results in the range error variance for the single sinusoid system as being

$$\sigma_r^2 = \frac{c^2 N_0}{2\pi^2 f_m^2 P_a^2 R^2 \tau_d} \tag{23}$$

As is also true in the present system, the range error variance of this system can be decreased by increasing the modulation frequency, f_m.

Reflectance Performance. In order to calculate the error variance of the reflectance estimate, Eq (12) can be used. The value to be used for the energy, E, in the received signal is the average power of the sinusoid, P_c, multiplied by the observation interval, τ_d. Thus,

$$E = \frac{P_a^2 R^2 \tau_d}{8} \tag{24}$$

and

$$\sigma_\rho^2 = \frac{4N_0}{P_a^2 R^2 \tau_d} \tag{25}$$

As can be seen, the modulating frequency has nothing to do with this error variance. The only way to decrease the variance is by either lengthening the observation interval or by increasing the laser power.

Resolution. The next performance characteristic to be considered is that of the system's resolution. Following the argument presented in the previous chapter, this resolution can be determined from the half-power width of the time autocorrelation function of the modulating signal. For a sinusoid, the time autocorrelation function is

$$R(\tau) = \cos 2\pi f_m \tau \tag{26}$$

After a little algebra, the distance between the half-power points is found to be

$$\tau_{res} = \frac{1}{4f_m} \tag{27}$$

where τ_{res} is the minimum resolvable time delay in seconds. Substituting Eq (27) into the basic relation

$$2R_{res} = c\tau_{res} \tag{28}$$

where R_{res} is the minimum resolvable distance, leads to the relation

$$R_{res} = \frac{c}{8f_m} \tag{29}$$

Thus, the higher the modulating frequency, the better the resolution. As an example, using a frequency of about 100 MHz, the system would be able to distinguish distances of approximately 1.2 feet. However, a frequency of 10 MHz would result in a resolution of only 12.3 feet. Although these figures provide a rough estimate of the resolution of the system, they are, as explained previously, worst-case estimates. A receiver operating at high signal-to-noise ratios should be able to distinguish objects which are much closer together than these figures would indicate.

Ambiguity. The final performance characteristic of interest is the ambiguity of the system. Since this system utilizes a harmonic tracking receiver, its ambiguity interval is identical to that of the present system. Thus, from Eq (19),

$$r_{amb} = \frac{c}{2f_m} \tag{19}$$

For a modulating frequency of 100 MHz, the ambiguity interval would be roughly five feet, whereas for a frequency of 10 MHz, it would be approximately 50 feet. Although decreasing f_m would solve the ambiguity problem, it would also degrade both the range estimation performance and the resolution of the system.

System Implementation. The last topic to be considered for the single sinusoid system is that of system implementation. For this system, implementation would be very easy. All of the required components are readily available, and the suggested system design is straightforward. Harmonic tracking is feasible, as proven by the present system.

However, there appears to be three areas which could cause a problem in the implementation of a single sinusoid system. The first one

is the bandwidth of the power detector. This bandwidth must be large enough to pass whatever frequency is being used as the modulating frequency, f_m. However, as has been shown, the higher the modulating frequency, the shorter the ambiguity interval. Thus, for an operational system, it is doubtful that f_m would ever be larger than the currently available detector bandwidth.

The second possible problem area is the selection of an appropriate modulating frequency such that the range, resolution, and ambiguity requirements can all be satisfied simultaneously.

Finally, the third area is one which is common to all scanner systems. The CW output of the laser must be large enough so that the received power is sufficient to keep the PLL above threshold. What this relates to in terms of actual power requirements will depend on the particular operational requirements of the system.

Linear Frequency Modulation

General Description. The next technique to be considered is one which utilizes a pulse compression technique which is commonly used in radar systems, that of linear frequency modulation (FM). In a linear FM pulse, also called a chirp pulse, the carrier frequency is linearly increased so that at the end of the pulse, it is Δf Hz higher than at the start (Fig 9, page 29). The chirp pulse is represented by the equation

$$s(t) = \cos[2\pi f_0 t + \frac{1}{2}\mu t^2] \qquad -\frac{T_p}{2} \leq t \leq \frac{T_p}{2} \qquad (30)$$

where T_p is the duration of the pulse and μ is a proportionality constant. The frequency deviation, Δf, is given by

$$\Delta f = \frac{\mu T_p}{2\pi} \tag{31}$$

As long as the time-bandwidth product, $T_p \Delta f$. is large, $T_p \Delta f \geq 20$, the frequency spectrum of the chirp is approximately rectangular with a total bandwidth of Δf Hz and is centered at what is called the carrier frequency, f_0 (Ref 2: 11-15).

When this FM pulse is passed through a properly matched filter in the receiver, it is compressed into a very narrow output pulse whose width is inversely proportional to the frequency deviation, Δf. This compression action greatly improves both the accuracy and the resolution of the system. Thus, the FM chirp is an ideal technique to use with peak-power limited transmitters, since the detection capability of long pulses (high transmitted energy) is combined with the accuracy and the resolution capability normally associated only with very narrow transmitted pulses.

The obvious method of applying the FM chirp technique to the laser scanner is by chirping the frequency of the laser itself. However, even

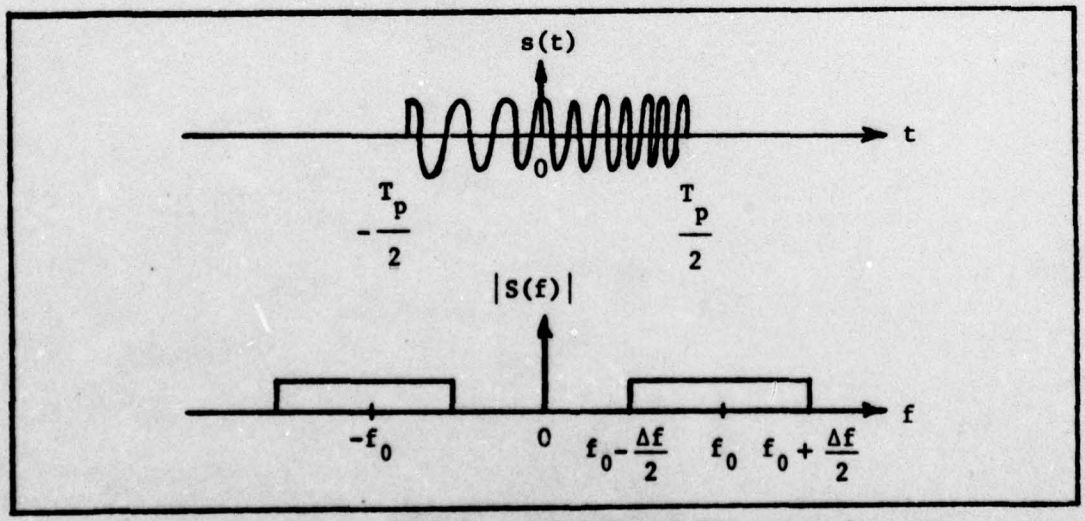

Figure 9. Linear FM Pulse and Related Frequency Spectrum

if this were possible, it would not be feasible for use with the proposed direct detection receiver. Therefore, an alternative method must be used which utilizes some type of subcarrier modulation. This can be easily accomplished by first generating an FM chirp pulse starting at some intermediate frequency, say 20 MHz, and then amplitude-modulating the output power of the laser with the chirped pulse.

Transmitter. A transmitter which will generate just such an output can be configured using either an active or a passive generation approach (Ref 2: 143-152). The active approach utilizes a signal generator whose output is a periodic ramp function (Fig 10, page 31). This linear signal drives a voltage-controlled oscillator (VCO) whose quiescent frequency is the desired starting frequency of the chirp. The duration and the slope of the ramp signal, along with the characteristics of the VCO, determine the frequency deviation, Δf, of the generated pulse. If required, a gating circuit which is synchronized with the signal generator can follow the VCO. Its output is thus a series of identical, linear FM pulses.

In order to determine the optimum length of these pulses, it is necessary to recall Eqs (5) and (12) from the previous chapter which showed that the accuracy of both the range and the reflectance estimates increases as the energy in the received signal increases. Thus, the longer the transmitted pulses, the more accurate the estimates. It has also been assumed that both range and reflectance are constant in a resolution cell. Therefore, the optimum situation is for each transmitted pulse to be τ_d seconds in length. This will permit maximum energy to be transmitted while still retaining the maximum horizontal resolution. This will also permit the gating circuit in the transmitter to be eliminated since the pulses will now be contiguous.

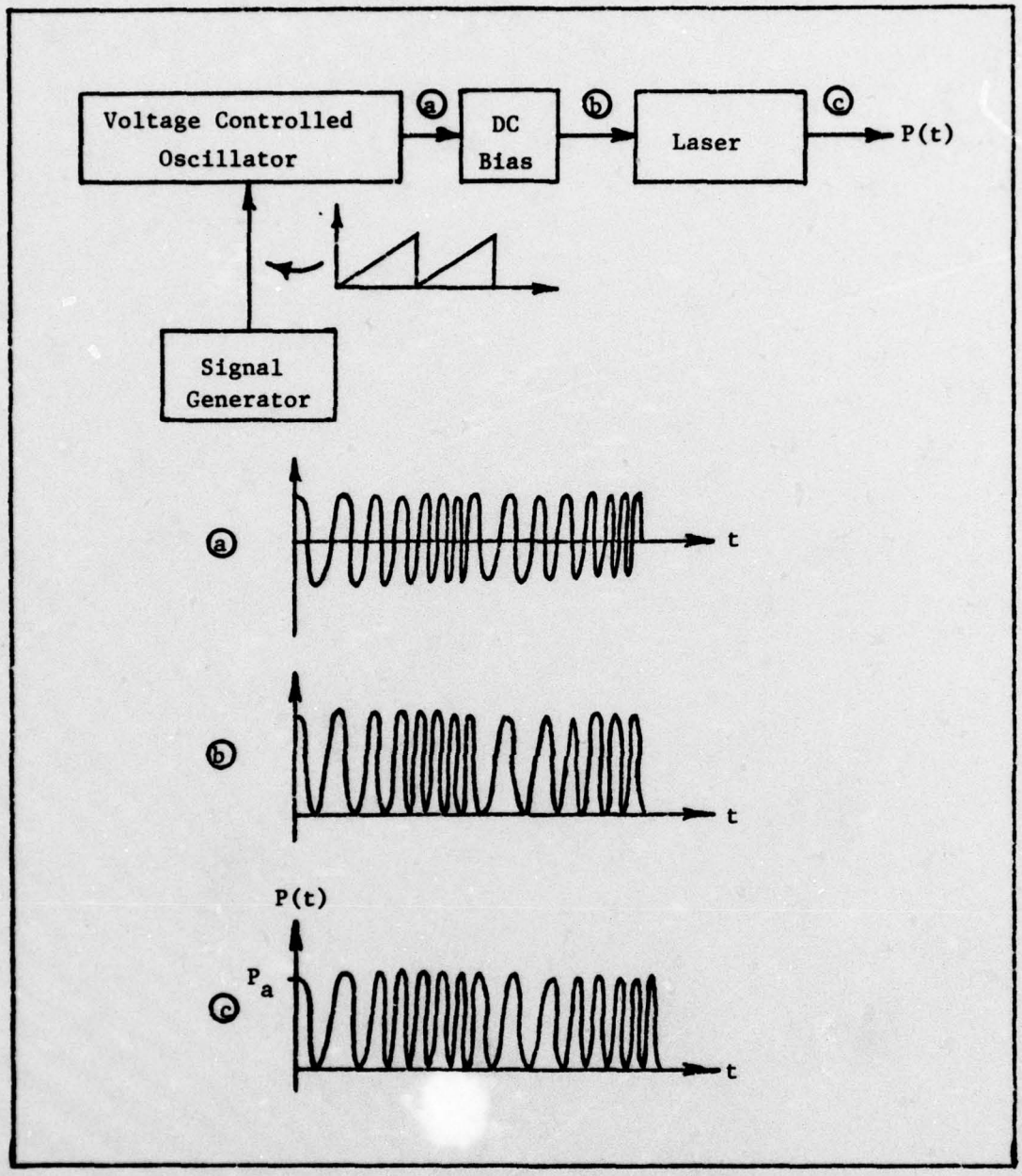

Figure 10. Active Chirp Transmitter with Associated Waveforms

A DC bias is added to the output of the VCO, and the resulting signal is used to excite the laser. The output power of the laser will thus be a series of contiguous pulses, each pulse of the form

$$P(t) = \frac{P_a}{2}\left[1 + \cos\left(2\pi f_0 t + \frac{1}{2}\mu t^2\right)\right] \qquad -\frac{\tau_d}{2} \le t \le \frac{\tau_d}{2} \tag{32}$$

where P_a is the CW power of the laser, μ is a proportionality constant which depends on the characteristics of the VCO, and τ_d is the time duration of each pulse.

The second type of transmitter utilizes a passive generation method (Fig 11, page 33). In this method, an impulse function is generated every τ_d seconds and is passed through an expansion filter. This filter, which has a linear time delay versus frequency characteristic, distorts the phase relationships of the various frequencies in the original impulse. The result is a stretching of the impulse into a much longer pulse which is very similar to an FM chirp pulse. It has been shown that the impulse function which comes the closes to generating the desired chirp is one of the form (Ref 2: 146-147)

$$s(t) = \frac{\sin\frac{\mu T_p t}{2}}{\frac{\mu T_p t}{2}} \cos 2\pi f_0 t \qquad (33)$$

where the desired pulse duration, T_p, is taken to be τ_d seconds. A DC bias is then added to the output of the expansion filter, and the laser is again excited by this resultant signal.

Receiver. As opposed to the two different methods of generating an FM chirp signal, there is only one feasible method of constructing a receiver to process the signal and to extract the desired information (Fig 12, page 34). The output of the power detector is first passed through a blocking capacitor, which eliminates the DC term. The remaining signal, which is identical to the linear FM pulse described in Eq (30), is then passed through a compression filter which is matched

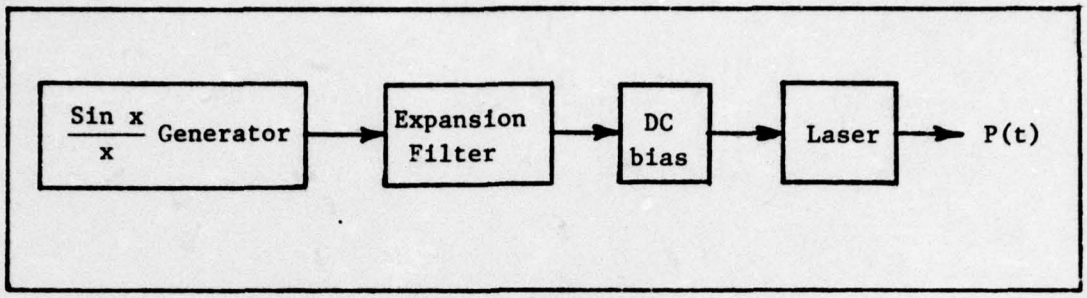

Figure 11. Passive Chirp Transmitter

to this signal. This compression filter has a time delay versus frequency characteristic of the opposite sense as the frequency sweep in the pulse. Thus, its frequency response is the conjugate of the frequency response of the expansion filter used in the passive generation transmitter.

The function of the compression filter is to again distort the relative phase relationships of the various frequencies in the signal. Only this time, the distortion results in a compression of the pulse back into its original sin x/x form. Thus, the output of the filter will be a very narrow pulse whose width is inversely proportional to the frequency deviation, Δf, of the FM pulse.

In order to generate the range estimate, the output of the matched filter is passed through a threshold detector which marks the time when the output exceeds a predetermined threshold. The relative time delay from the beginning of the current τ_d second interval is then calculated and is converted to a slant range estimate by an amplifier following the detector. This range estimate is then combined with the range correction signal in order to produce the corrected estimate of the target's slant range from the scanner. A reflectance estimate is also calculated from the matched filter output by choosing the peak value of the output every time a range estimate is generated. This value corresponds to the maximum-likelihood estimate of the actual reflectance value.

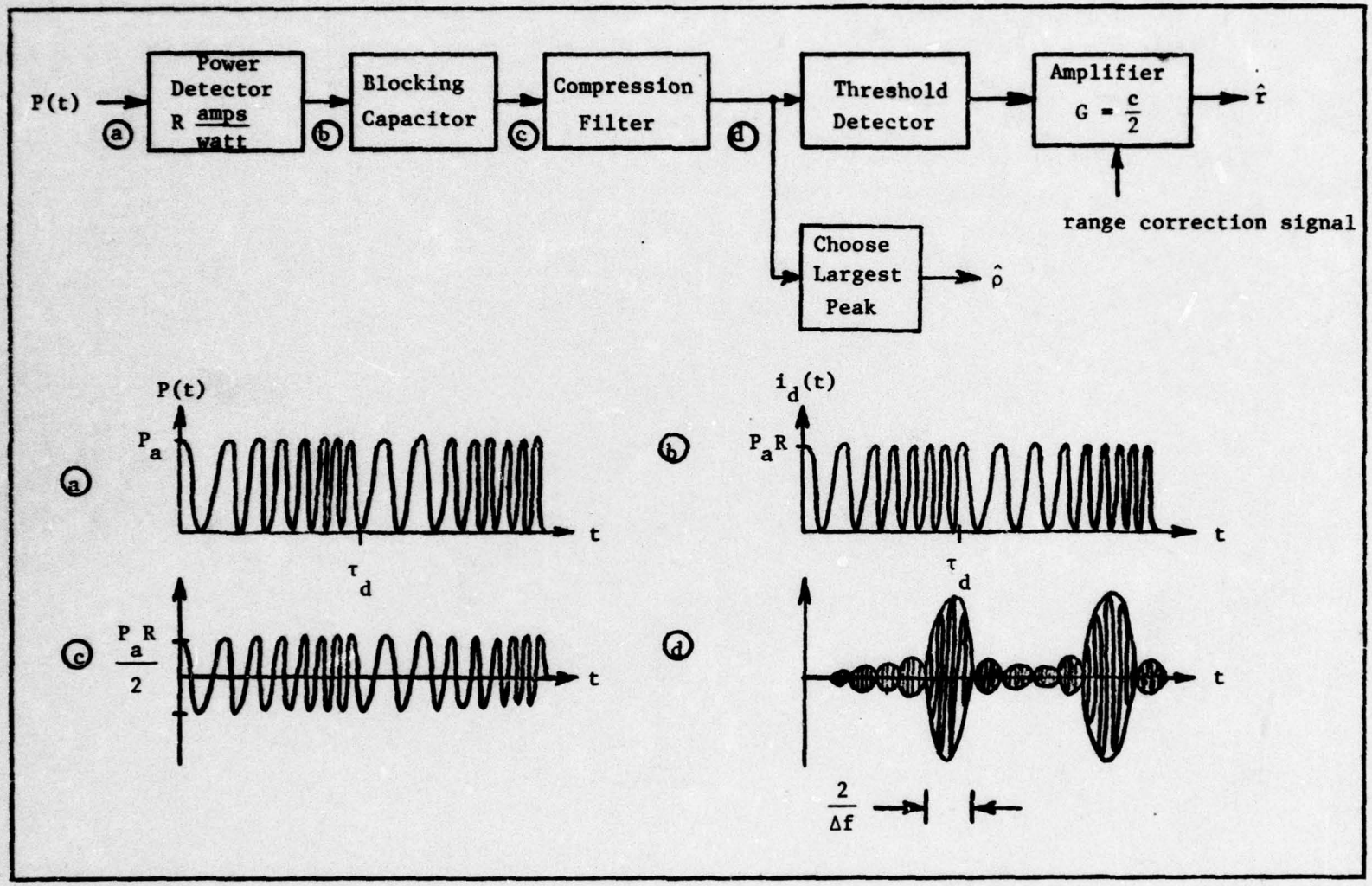

Figure 12. Receiver Structure and Related Waveforms for a Linear FM System

Range Performance. Based on the preceding description of the system configuration, an analysis of the system performance can now be conducted. The first item of interest is the accuracy of the range estimate provided by the receiver. Eq (5), which gives an expression for the error variance of the range estimate in a matched filter receiver, is applicable to the FM chirp system. The two variables which must first be calculated before this equation can be used are the received energy, E, and the mean-squared bandwidth, β^2. Since the input to the matched filter is an FM pulse of amplitude $P_a R/2$ and duration τ_d seconds, the received energy is

$$E = \frac{\left(\frac{P_a R}{2}\right)^2}{2} \tau_d = \frac{P_a{}^2 R^2 \tau_d}{8} \tag{34}$$

Also, for large time-bandwidth products, $\tau_d \Delta f \geq 20$, the value of the mean-squared bandwidth has been calculated to be (Ref 2: 302-304):

$$\beta^2 = \frac{\pi^2 \Delta f^2}{3} \tag{35}$$

Thus, substituting these values into Eq (5), the error variance of the range estimate for the FM chirp system becomes

$$\sigma_r{}^2 = \frac{3c^2 N_0}{\pi^2 \Delta f^2 P_a{}^2 R^2 \tau_d} \tag{36}$$

As can be seen from Eq (36), the accuracy of the FM chirp system can be increased by either increasing the frequency deviation, Δf, of the signal, or by increasing the received energy, i.e., increasing either the received power, P_a, or the pulse duration, τ_d.

The range error variance derived by using a leading-edge analysis turns out to be higher than the variance found above by a factor of approximately 1.9. The derivation of this variance is provided in Appendix A.

Reflectance Performance. The next characteristic of the system performance to be considered is that of the accuracy of the reflectance estimate. Eq (12), which gives an expression for the reflectance error variance in a matched filter system, can be used to find this accuracy. Substituting the expression for the received energy given by Eq (34) into Eq (12) results in the error variance of the reflectance estimate for the FM chirp system as being

$$\sigma_\rho^2 = \frac{4N_0}{P_a^2 R^2 \tau_d} \tag{37}$$

Again, this variance can be decreased by either increasing P_a or τ_d, which is equivalent to increasing the received energy per resolution cell.

Resolution. Another characteristic of the system which is of interest is its resolution capability. As shown previously, the output of the compression filter in the receiver is of the form of a sin x/x pulse whose main lobe has a total width of $2/\Delta f$ seconds. Thus, the half-power width, which corresponds to the time resolution of the system, is calculated to be

$$\tau_{res} = \frac{0.9}{\Delta f} \tag{38}$$

Changing this to a range resolution results in

$$R_{res} = \frac{0.45c}{\Delta f} \tag{39}$$

As an example, a Δf of 10 MHz would result in a resolution of 44 feet, a Δf of 100 MHz would lead to a 4.4 foot resolution, and a Δf of 1 Gigahertz (GHz) would have a 0.4 foot resolution capability.

Ambiguity. The final characteristic of the system to be considered is that of its ambiguity. Since the period of the modulating signal is τ_d seconds, the range ambiguity interval is found from Eq (19) to be

$$r_{amb} = \frac{c\tau_d}{2} \tag{40}$$

For a dwell time of 1.59 microseconds, as in the existing system, the ambiguity interval turns out to be approximately 782 feet, much larger than needed for tactical-sized targets. For a smaller dwell time of 0.33 microseconds, the ambiguity interval is 162 feet. Whether or not this interval is large enough depends on the targets of interest. In order to increase the ambiguity interval, the period of the transmitted signal must be increased. Although this can be done fairly easy, it would also result in a degradation of the horizontal resolution of the system.

System Implementation. Now that the system configuration has been described and the important performance characteristics analyzed, it is time to take a brief look at some of the qualitative aspects of implementing an FM chirp system.

To begin with, the output of the compression filter in the receiver consists of time sidelobes as well as the mainlobe. The magnitude of the sidelobe adjacent to the mainlobe is only 13.2 decibles (db) down

from the amplitude of the mainlobe. The amplitudes of the remaining sidelobes decrease very slowly, with the first several decreasing at a rate of about 4 db per sidelobe (Ref 2: 173). This could cause a problem if the noise in the receiver were to consistently cause the magnitude of the sidelobes to exceed the threshold value, thus resulting in an erroneous time measurement. This is the global accuracy problem discussed in the preceding chapter. However, it is possible to reduce the level of these sidelobes by additional filtering, called weighting, of the signal (Ref 9: 4). Many different weighting methods have been developed to deal with the sidelobe problem, but all of these cause a slight degradation of 1 to 2 db in the signal-to-noise ratio of the signal (Ref 9: 26-35). In addition, they cause a widening of the mainlobe, thus degrading the resolution of the system. The amount of this widening depends on both the type and the amount of weighting used (Ref 2: 201). Thus, the use of a weighting filter in a particular system must depend on the seriousness of the sidelobe problem in that particular system.

Another item of interest can be called the feasibility of using an FM chirp system. Since the FM chirp technique is widely used in radar systems, the matched filter technology is well developed. Both expansion and compression filters are available with a wide variety of characteristics and in a wide variety of types, such as strip delay lines and surface-wave delay lines (Ref 9: 4-13). Recent developments in surface-wave technology have produced filters which can generate an FM chirp pulse with a center frequency of 1.3 GHz, a frequency deviation of 500 MHz, and a total pulse duration of approximately 2 microseconds (Ref 10: 695-698).

However, the major problem that would be encountered would be in the modulating of the laser. As explained previously, the time-bandwidth product, $\tau_d \Delta f$, must be greater than 20 in order for both the approximate frequency spectrum of the chirp pulse (Fig 9, page 29) and the value of its mean-squared bandwidth (Eq (35)) to be valid. In order to meet this requirement, the frequency deviation must be at least 10 MHz for the present dwell time. Current device technology of both VCO's and expansion filters limits the value of Δf to approximately one-half of the starting frequency of the chirp (Ref 9: 4-15, Ref 10: 695-698). Thus, for a Δf of 10 MHz, the starting frequency must be at least 20 MHz, and the highest frequency in the chirp pulse would be 30 MHz (Fig 9, page 29).

However, in an operational system, requirements for the accuracy of the range estimate and for the resolution of the system (both dependent upon Δf) would probably dictate a much higher value of Δf, resulting in a correspondingly higher starting frequency. The highest frequency in the chirp pulse in such a system could conceivably be in the Gigahertz (GHz) region. Thus, the problem would be how high a frequency can a semi-conductor laser be modulated before it becomes inoperable. A recent study has shown that a 25 MHz modulation rate is easily obtainable with currently-available semiconductor lasers (Ref 1: 1-14). However, this study did not attempt to determine the maximum modulation rate achievable. If this maximum rate does not turn out to be high enough for operational requirements, further developmental work in laser modulation may be required before an FM chirp system becomes feasible.

A final item of interest is the required detector bandwidth. The detector will have to have at least a bandwidth equivalent to the highest

frequency in the chirp pulse. At a minimum, this would be approximately 30 MHz. At a maximum, it again could be over 1 GHz. Thus, the FM chirp system trades bandwidth for performance. The greater the available bandwidth, the better the system performance.

Pseudonoise Coding

General Description. The third technique to be considered is another pulse compression technique that is used in radar systems, that of pseudonoise (PN) coding of the transmitted signal. In a PN coded system, the transmitted sinusoid is divided up into a number of short intervals, each of width t_0 seconds, called the chip width. The phase of the sinusoid in each interval is determined by the value of the PN code in that interval. Since a PN code is a periodic, binary code, the values of the periodic binary waveform corresponding to the code can be set to ± 1. Thus, the phase of the sinusoid in each interval will be either 0 degrees or 180 degrees and will alternate in each interval in accordance with the PN code (Fig 13, page 41).

The binary sequence from which a PN binary waveform is derived can be easily generated by means of a linear shift register with appropriate feedback connections. Since the details of such a code generator are discussed extensively in the literature, they will not be repeated here (Ref 5: 145-148). However, several important characteristics of the coded binary waveform which are of interest will be summarized. To begin with, the length of the code, i.e., the number of chip widths in the code before it begins to repeat, is dependent on the number of stages in the generating shift register. If the shift register has N stages, the length of the code, p, will be 2^N-1. Since each chip is of

duration t_0 seconds, the total time duration of the code before it repeats is pt_0 seconds.

Another important characteristic is that the number of intervals in which the binary waveform has a value of plus one is given by $(p+1)/2$, while the number of intervals in which it is minus one is given by $(p-1)/2$. Thus, there will be one more plus one than minus one in the code. Finally, the time autocorrelation function of a periodic PN code which is normalized with respect to the energy in one code word duration, pt_0 seconds, consists of a mainlobe, which peaks at a value of one, and a sidelobe which has a constant value of $(-1/p)$ (Fig 14, page 42). The derivation of this autocorrelation function assumes that the code has a period of pt_0 seconds, i.e., that the code words are contiguous. This autocorrelation function can be generated by a filter which is matched to the complete pt_0-second code word. When the current code word has been received, the output of the filter will peak as does the

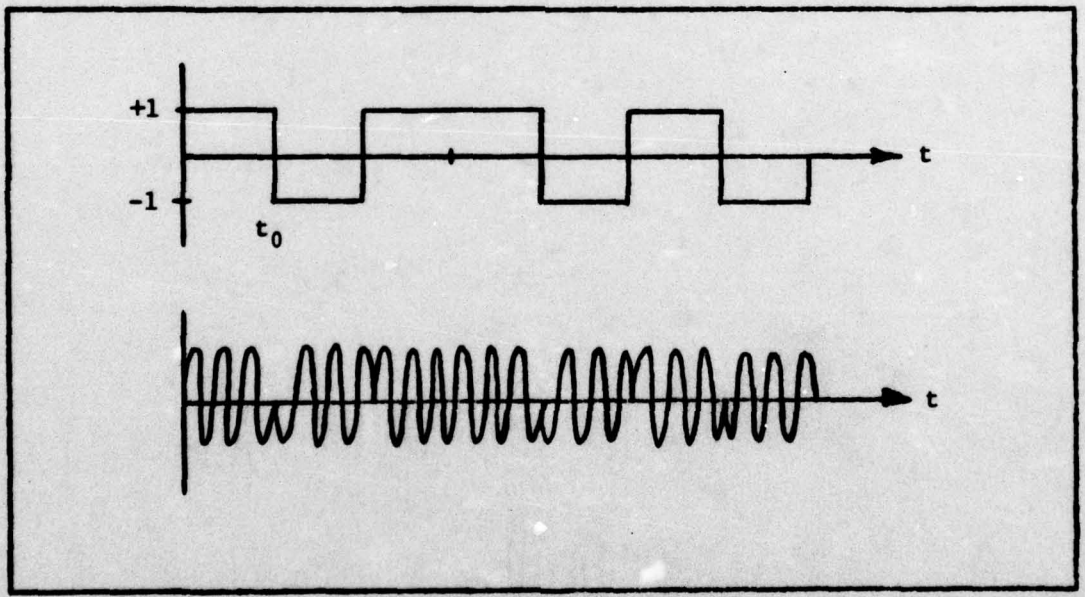

Figure 13. Typical PN Coded Waveform and Resulting Phase-Coded Sinusoid

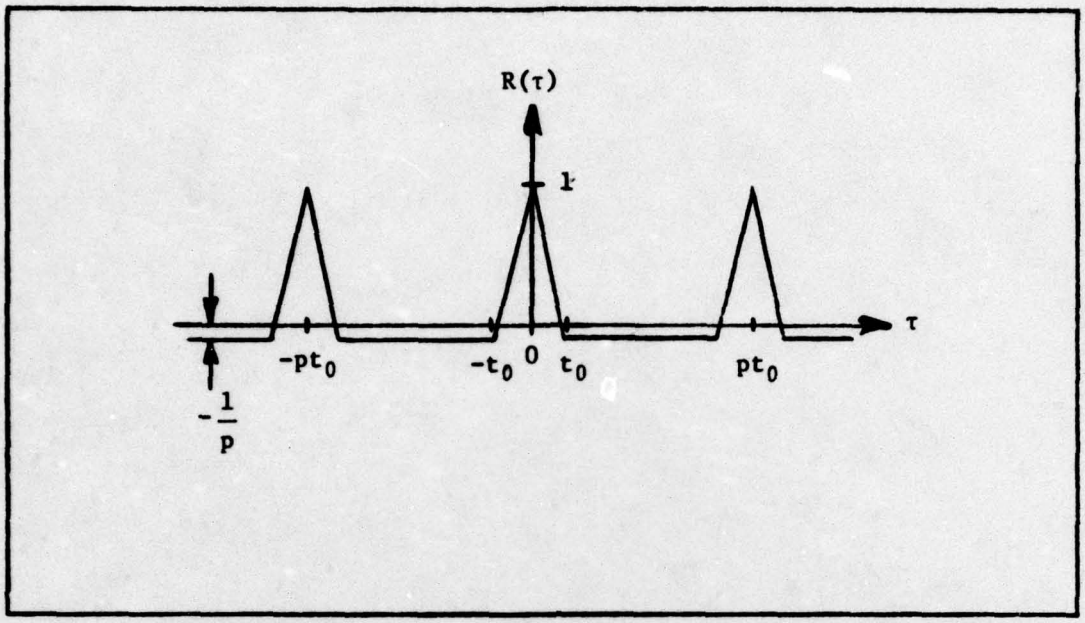

Figure 14. Time Autocorrelation Function of a Periodic PN Waveform

autocorrelation function. However, at all other times, i.e., before the current code word has been completely received, and while parts of the previous code word are still within the delay line, the output will exhibit the negative sidelobes of the autocorrelation function. Also, since the code is periodic, the autocorrelation function is also periodic, with a period of pt_0 seconds (Ref 5: 148-149).

The technique of coding a signal with a PN code can be adapted to the laser scanner system in the same way as the FM chirp technique; that is, by subcarrier modulation. Thus, a sinusoid at an intermediate frequency can first be phase-coded by a PN code, and the resulting signal used to amplitude-modulate the output power of the laser.

Transmitter. A transmitter which will generate just such an output can be easily constructed (Fig 15, page 43). A waveform generator, the output of which is the PN coded binary waveform, is used to modulate a sinusoid of frequency f_m. The resulting signal is the phase-coded

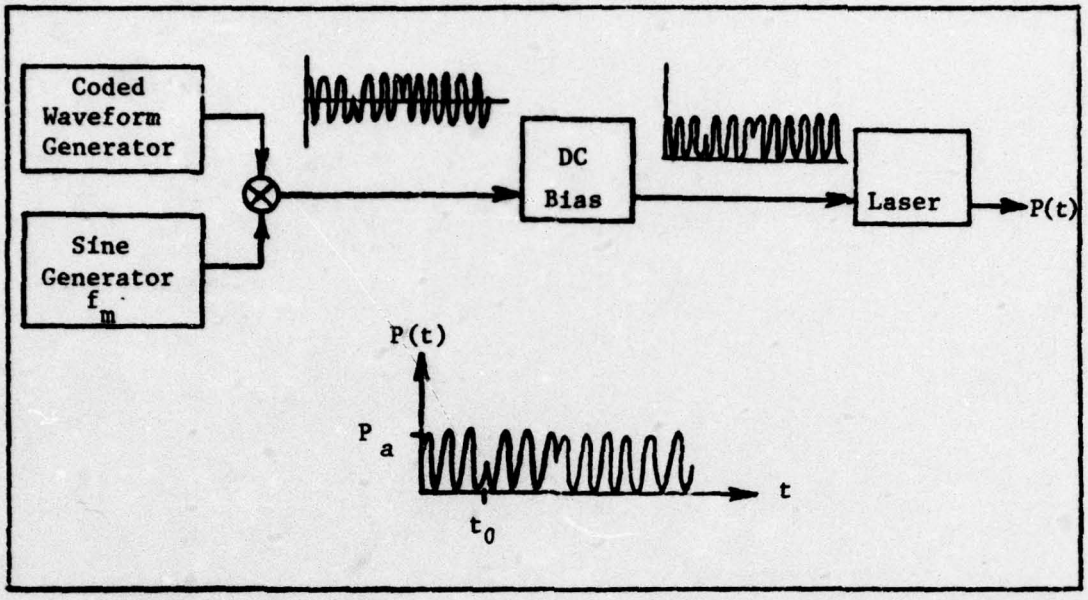

Figure 15. Transmitter Structure for a PN Coded System

sinusoid described above (Fig 13, page 41). By adding a DC bias to this signal and using the resulting signal to excite the laser, the output power of the laser, P(t), will have the desired amplitude modulation. The laser output for each code duration can be represented as

$$P(t) = \frac{P_a}{2} + \frac{P_a}{2} \sum_{i=0}^{p-1} a_i \sin 2\pi f_m t\{U(t-it_0)-U[t-(i+1)t_0]\} \quad 0 \leq t \leq \tau_d \quad (41)$$

where $a_i = \{\pm 1\}$, and U(t) is the unit step function.

As was the case in the FM chirp system, it is also desirable in this system to maximize the energy transmitted in each dwell time in order to minimize the error variances of the range and reflectance estimates. Also, as mentioned earlier, the code words must be transmitted contiguously in order to achieve the low sidelobes of the autocorrelation function. Thus, the length of the code, p, and the chip width, t_0, can be chosen so that the time duration of each code,

pt_0, is equal to the dwell time, τ_d seconds. The transmitter output will then be a continuous coded signal which repeats every τ_d seconds.

Receiver. The receiver for a PN coded system is slightly more complicated than the transmitter just described. The received optical signal, P(t), is first detected by the optical detector, which converts it to an electrical current (Fig 16, page 45). A blocking capacitor eliminates the DC term so that the resulting signal is a typical phase-coded sinusoid. This sinusoid is then sent into a tapped delay line which has a total of p taps and where the delay between taps is equal to t_0 seconds.

The output at each of these taps is multiplied by the appropriate value, either ± 1, and then sent into a summing network. These p multipliers are set equal to the transmitted PN code, with the first code bit being placed into the multiplier at the last tap on the delay line. The result of this delay line-summer network is that when the current code word has been received, i.e., it is completely within the delay line, it is, in effect, decoded by the multipliers, so that the output of each multiplier is a sinusoid with a phase angle of zero degrees. Since all of these outputs are in phase, they add together in the summer, forming one sinusoid whose amplitude is p times the original amplitude. The duration of this in-phase signal is t_0 seconds, since after this time duration the current code word is being shifted out of the delay line and is being replaced by the next code word. Due to the characteristics of a PN code, all other combinations of code bits in the delay line will result in destructive addition in the summer, and the resultant summer output will be a single amplitude sinusoid with a phase angle of 180 degrees.

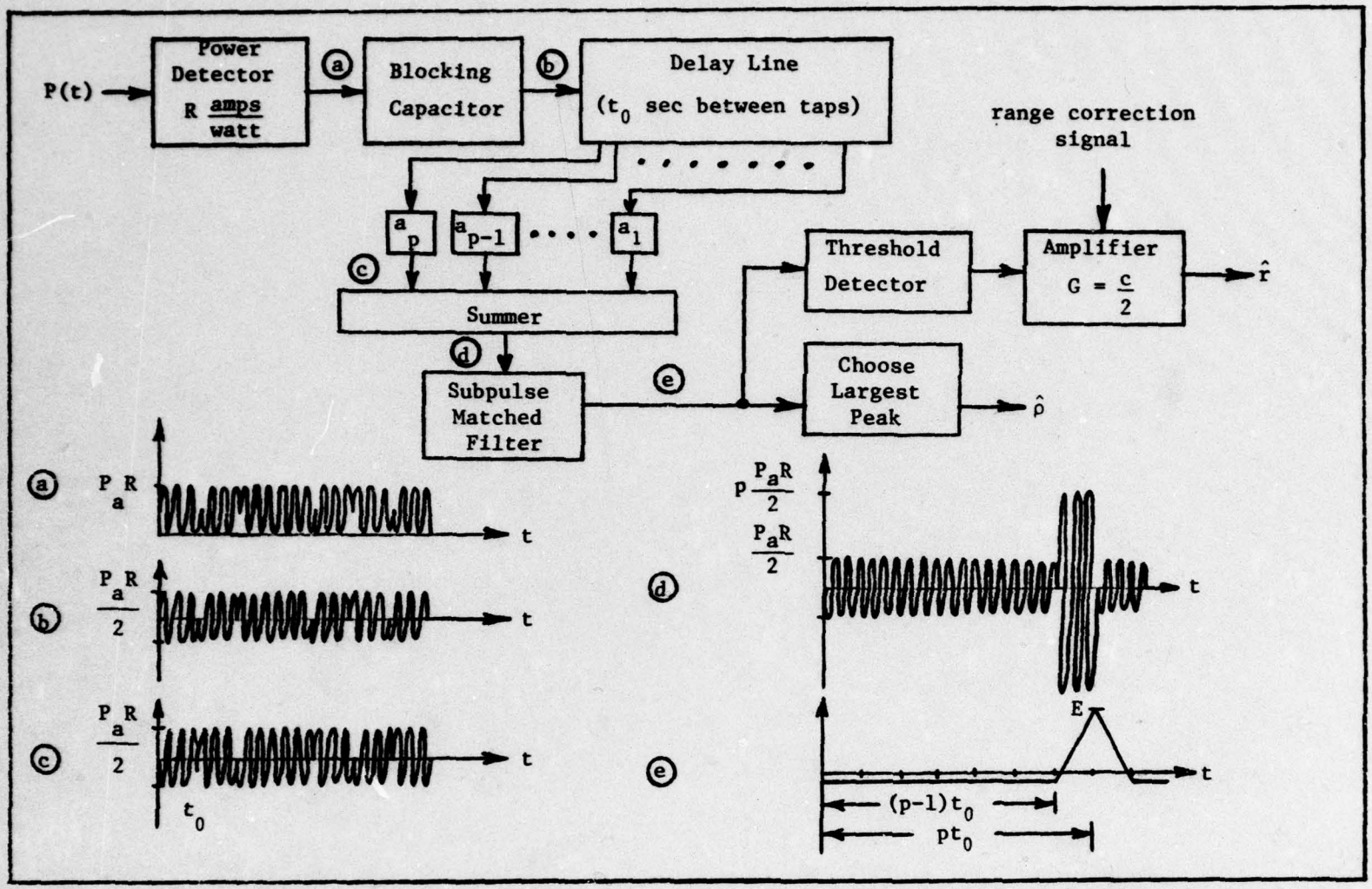

Figure 16. Receiver Structure and Associated Waveforms for a PN Coded System (Waveforms assume that the system has been operating for at least pt_0 seconds.)

The output of this summing network is routed through a filter which is matched to the t_0 second chip width of the signal. As long as the summer output is the continuous sinusoid with a 180° phase angle, the output of this filter will be a constant negative current. However, when the summer output is the in-phase signal resulting from the reception of the complete code word, the output of the filter will be the sharp peak corresponding to the mainlobe of the time-autocorrelation function of the PN code. Thus, the receiver has compressed the long transmitted pulse, p code bits long, into a very narrow output peak whose width is dependent only on the size of the chip width, t_0, and whose peak value is proportional to the energy contained in the entire τ_d second pulse.

The output of the matched filter is processed in the same manner as in the FM chirp system. Thus, in order to measure the slant range from the scanner to the target, the output is routed through a threshold detector which is triggered when the output peaks. The time delay thus measured is then converted to a slant range estimate by an amplifier following the threshold detector. The reflectance is estimated simply by noting the peak value of the filter output in every τ_d second interval. Since this value is proportional to the total received energy, it gives the desired reflectance estimate.

Range Performance. Now that the system configuration has been described, the performance of the system can be analyzed. To begin with, the error variance of the range estimate will again be calculated by using Eq (5), the expression for a matched filter receiver. For the PN coded system, the energy in one complete code word of τ_d seconds is given by

$$E = \frac{\left(\frac{P_a R}{2}\right)^2}{2} \tau_d = \frac{P_a^2 R^2 \tau_d}{8} \tag{42}$$

Also, the mean-squared bandwidth of the signal, β^2, can be calculated to be (reference Appendix B)

$$\beta^2 = \frac{4(p+1)}{\pi p t_0^2} \tag{43}$$

Substituting Eqs (42) and (43) into Eq (5) results in the expression for the range variance for a PN system:

$$\sigma_r^2 = \frac{\pi c^2 N_0 t_0}{4 P_a^2 R^2 (p+1)} \tag{44}$$

Thus, the range error variance shows a dependence on both p and t_0. However, it has been specified that the product pt_0 is a constant for a given dwell time. Thus, the range error variance can be decreased by decreasing the chip width, t_0, while simultaneously increasing the code length, p. A comparison of this error variance with the variance computed using the leading-edge analysis shows that the leading-edge variance is higher by a factor of only 1.3 (reference Appendix C).

Reflectance Performance. The next system characteristic of interest is the error variance of the reflectance estimate. This variance can be found for the PN system by using Eq (12). Substituting the value for the received energy given by Eq (42) into Eq (12) results in

$$\sigma_\rho^2 = \frac{4N_0}{P_a^2 R^2 \tau_d} \tag{45}$$

Thus, the reflectance performance can be improved only by increasing either the received power or the dwell time of the scanner.

Resolution. The resolution capability of a PN system can also be found based on the previously presented results. Since the time resolution of the system is calculated from the half-power width of the mainlobe of the time autocorrelation function of the modulating signal, the time resolution of the PN system is found to be

$$\tau_{res} = 0.6t_0 \tag{46}$$

This equates to a range resolution of

$$R_{res} = 0.3ct_0 \tag{47}$$

As an example, for a chip width of 10 nanoseconds, the system resolution is roughly 3 feet. Decreasing t_0 to 5 nanoseconds results in a resolution of approximately 1.5 feet, while decreasing it even further to 2 nanoseconds improves the resolution to 0.6 feet.

Ambiguity. The final characteristic of interest is the ambiguity of the system. Since the PN coded signal is periodic with a period of τ_d seconds, Eq (19) is valid, and

$$r_{amb} = \frac{c\tau_d}{2} \tag{48}$$

Thus, the ambiguity of the PN system is identical to that of the FM chirp system. As in the chirp system, the ambiguity interval for the dwell time of 1.59 microseconds being used in the present system is calculated to be 782 feet.

System Implementation. Now that the performance of a PN system has been considered, a few comments will be made concerning its implementation and feasibility. To begin with, since the output of the matched filter has only a sharply peaked mainlobe and a sidelobe which has a constant negative value, the global accuracy problem discussed in the preceding chapter is nonexistant.

Another item of interest is the availability of components. In order to obtain good resolution capabilities, the chip width, t_0, must be on the order of 5 nanoseconds or less. This would mean that the code generator would have to be capable of generating its code bits at a rate of 200 Megabits per second or greater. This rate may be too high for a code generator which uses a linear shift register. However an alternate method of generation has been under development for several years. This method, which uses a surface acoustic wave device, is reported to be capable of bit rates up to 300 Megabits/sec (Ref 11: 224).

Device technology is also a consideration for the receiver components. The delay line must have a large number of taps and a total delay of τ_d seconds. For chip widths on the order of nanoseconds, the code length, p, would be several hundred, based on the present dwell time. Even for a much smaller dwell time of 0.33 microseconds, p would still be on the order of one hundred. However, it appears that this will not be a major problem. Development of delay lines using surface-wave technology is continuing and should result in devices capable of meeting the requirements of the scanner system (Ref 12: 186-187).

A third item of interest in the implementation of a PN system is the actual modulation of the laser. As in the FM chirp system, this

would be the major problem that would be encountered in the implementation of the system. In order to have several cycles of the subcarrier sinusoid contained within each chip width, the frequency of this sinusoid, f_m, will have to be in the Gigahertz region. Whether or not a semiconductor laser can be modulated at such a high rate remains to be determined, as has previously been discussed. If such a high frequency is not obtainable, a lower frequency could be used, with the result that the chip width would have to be increased. Although this might not significantly degrade the range and reflectance error variances of the system, it could degrade its resolution capability to an unacceptable level.

The final item of interest is the problem of the required detector bandwidth. Since the binary waveform is used to modulate a sinusoid of frequency f_m, the resulting spectrum will be centered around f_m, and its upper limit can be taken as $f_m + 2/t_0$ (Fig 23, page 86). Since f_m must be greater than $(1/t_0)$, the bandwidth required for t_0 to be in the nanosecond range can easily be greater than one Gigahertz. Thus, as is also true of the FM chirp system, the PN system trades bandwidth for performance. The greater the available bandwidth, the better the performance of the system.

Pseudonoise Coded On-Off System

General Description. The final modulation technique to be discussed is a variation of the pseudonoise-coded subcarrier system considered in the preceding section. In particular, this technique eliminates the subcarrier, and modulates the laser directly with the coded binary waveform. The resulting output of the laser in each chip width is thus

either on or off, depending upon the value of the code in that particular interval.

The transmitter for this on-off system is very similar to the transmitter for the subcarrier PN system. A DC bias is first added to the output of a coded waveform generator, and the resulting signal is used to excite the laser (Fig 17, below). The output power of the laser for each code duration of τ_d seconds can be represented by the equation

$$P(t) = \frac{P_a}{2} + \frac{P_a}{2} \sum_{i=0}^{p-1} a_i\{U(t - it_0) - U[t-(i+1)t_0]\} \qquad 0 \le t \le \tau_d \qquad (49)$$

where $a_i = \{\pm 1\}$, and U(t) is the unit step function.

The receiver structure for this system is identical to the structure used for the subcarrier PN system. The received optical signal, P(t), is first detected by a power detector and converted into an electrical current (Fig 18, page 52). A blocking capacitor eliminates the DC term, and the resulting signal is sent into a delay line-summer network.

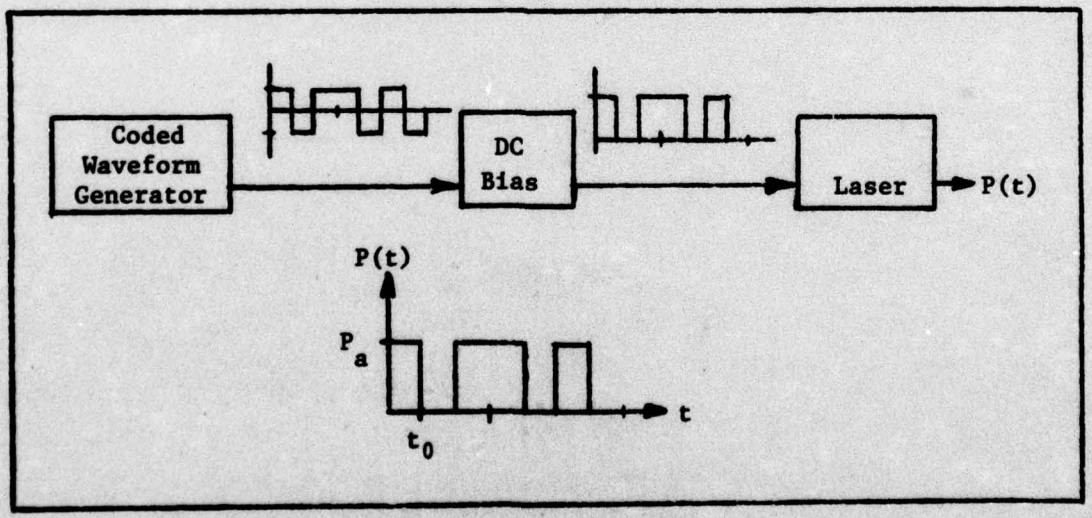

Figure 17. Transmitter for a PN Coded On-Off System

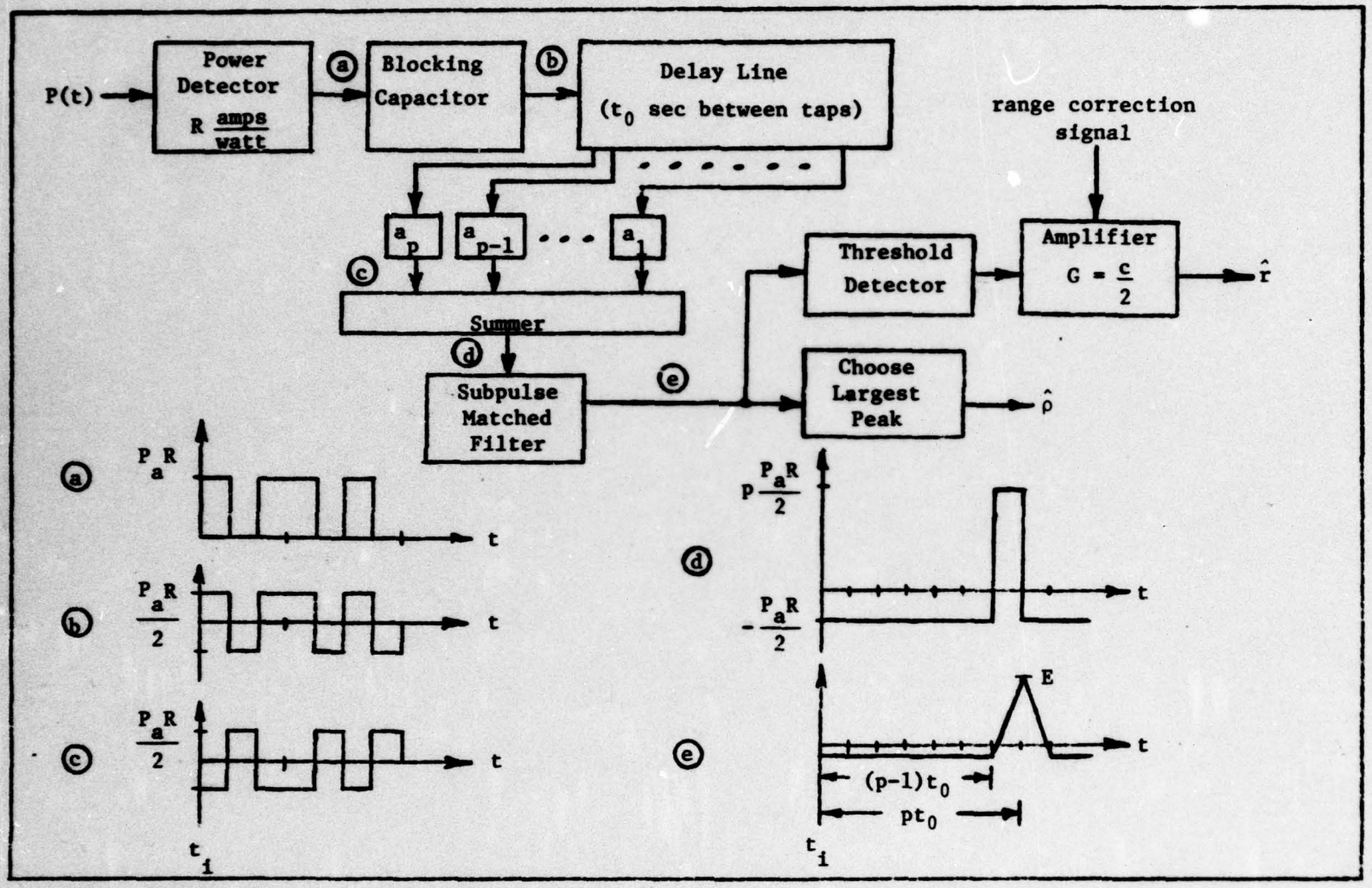

Figure 18. Receiver Structure and Associated Waveforms for a PN Coded On-Off System (Waveforms assume that the system has been operating for at least pt_0 seconds.)

The operation of the delay line-summer network is exactly the same as explained previously. The output of the network will be a constant negative value as long as the current code word is not completely within the delay line. However, when the current code word has been received, the output will peak for t_0 seconds, since all of the individual outputs of the multipliers will be in phase. The output of this network is routed through a filter which is matched to the subpulses. The output of this matched filter is then processed as in the previous matched filter system. A threshold detector first detects the output peaks and measures the time delay information. An amplifier following this detector then converts the time delay into the desired slant range estimate. The reflectance estimate is again generated simply by choosing the peak value of the matched filter output every time a range estimate is generated.

Range Performance. Based on the preceding system configuration, the performance characteristics can now be derived. The range performance is again derived using Eq (5). For this system, the energy is found to be

$$E = \left(\frac{P_a R}{2} \right)^2 \tau_d = \frac{P_a^2 R^2 \tau_d}{4} \tag{50}$$

Comparison of this equation with Eq (42) shows that the received energy in this system is twice as large as that in the PN subcarrier system. This difference is due simply to the difference in energy between a sinusoid and a square wave which have the same amplitude. Since the signal modulation in this system is the same binary waveform as in the subcarrier system, the value for the mean-squared bandwidth derived in

Appendix B is also valid for this system. Thus,

$$\beta^2 = \frac{4(p+1)}{\pi p t_0^2} \tag{43}$$

and the error variance of the range estimate is found to be

$$\sigma_r^2 = \frac{\pi c^2 N_0 t_0}{8 P_a^2 R^2 (p+1)} \tag{51}$$

As expected, the accuracy can again be increased by decreasing the chip width, t_0, and increasing the code length, p.

Reflectance Performance. The reflectance performance of the system can again be derived by use of Eq (12). Substituting Eq (50) into Eq (12) results in the error variance of the reflectance estimate:

$$\sigma_\rho^2 = \frac{2N_0}{P_a^2 R^2 \tau_d} \tag{52}$$

The reflectance performance can again be improved only by increasing the received energy.

Resolution. The resolution of the system depends only on the time autocorrelation function of the modulating signal. Since the modulating signal for this system is the same as that used in the subcarrier PN system, the resolution properties of the two systems are identical. Thus, the resolution of this system is given by

$$R_{res} = 0.3ct_0 \tag{47}$$

Ambiguity. The final system characteristic, its ambiguity, depends only on the period of the modulating signal. Thus, the ambiguity interval

for this system is identical to that of the PN subcarrier system, and

$$r_{amb} = \frac{c\tau_d}{2} \tag{48}$$

System Implementation. The final item of interest is, of course, that of system implementation. In general, the implementation issues for this system are identical to those of the subcarrier PN system. Since the time-autocorrelation functions are the same, the global accuracy analysis is the same. Also since the coded waveform generators and the delay line-summer networks have the same characteristics, the problem of device technology and availability parallels that already discussed.

However, there are two major differences between the systems which make the on-off system easier to implement. The first difference is in the modulation of the laser. Since there is no subcarrier sinusoid in the on-off system, the laser is modulated at the frequency of the binary waveform generator. Thus, it will have to be capable of being modulated at a rate of $(1/t_0)$ Hz. For a chip width of 5 nanoseconds, this would only be a rate of 200 MHz, about a factor of 3 less than the rate that the PN subcarrier system would require.

The second difference is in the required detector bandwidth. For the on-off system, the required bandwidth is approximately $(2/t_0)$ Hz. Thus, a chip width of 5 nanoseconds would require a bandwidth of approximately 400 MHz. This would again be a significant improvement over the PN subcarrier system, this time by a factor of about four.

However, this revised PN system still requires large bandwidths for good performance. As in all of the matched filter systems discussed,

the performance of this system can be improved only by increasing the bandwidth of the transmitted signal.

IV. Comparisons of Proposed Systems

Having completely described and analyzed each of the four proposed modulation techniques, the next step is to compare them. The basis of comparison to be used will be that of the range and the reflectance performance of the systems. In particular, expressions will be derived in this chapter which relate the standard deviations of the range and the reflectance errors of the two systems being compared. This standard deviation measure is just the square root of the error variances already derived. In addition, the resolution capabilities of the systems, their ambiguity intervals, and their ease of implementation will also be compared. In carrying out this comparison, it will be assumed that the values of P_a, the CW output power of the laser, R, the responsivity of the power detector, and N_0, the power spectral density of the noise, are identical in each of the systems being compared.

In order to simplify the system comparisons, only one of the pseudo-noise systems will be included. A visual comparison of Eqs (44) and (51) and Eqs (45) and (52) shows that the PN coded on-off system is better than the PN subcarrier system by a factor of two in both the range and the reflectance error variances. In addition, it was shown that a PN on-off system would be easier to implement. Therefore, since there does not seem to be any advantage to using a PN subcarrier system, only the PN on-off system will be included in the comparisons.

PN On-Off System and FM Chirp System

Range Comparison. The first comparison is between the PN on-off system and the FM chirp system. In order to compare the range performance of the two systems, Eqs (36) and (51) can be combined algebraically,

resulting in the equation

$$\sigma_{rPN} = 1.1\,\Delta f t_0 \sigma_{rFM} \tag{53}$$

where σ_{rPN} and σ_{rFM} are the standard deviations of the range error for the PN on-off system and FM chirp system, respectively.

In order to obtain a realistic comparison of the systems, it will be assumed that the bandwidth of the power detector has an upper limit of W Hz. It will also be assumed that the following relations are valid:

$$t_0 = \frac{2}{W} \tag{54}$$

and

$$f_1 + \Delta f = W \tag{55}$$

where f_1 is the starting frequency of the FM chirp pulse (Fig 9, page 29). In addition, it has been required that $\Delta f \leq f_1/2$ due to device limitations. Therefore, assuming the best case of $\Delta f = f_1/2$, Eq (55) can be written as

$$\Delta f = W/3 \tag{56}$$

Substituting Eqs (54) and (56) into Eq (53) results in

$$\sigma_{rPN} = 0.73\,\sigma_{rFM} \tag{57}$$

Eq (57) states that, assuming a detector bandwidth restriction, the PN on-off system will always outperform the FM chirp system by a factor of roughly 1.4.

Reflectance Comparison. In order to compare the reflectance performance of the two systems, Eqs (37) and (52) can be combined, resulting in

$$\sigma_{\rho PN} = \frac{1}{\sqrt{2}} \sigma_{\rho FM} \tag{58}$$

Eq (58) states that the reflectance performance of the PN system will always be better than that of the FM system, by a factor of $\sqrt{2}$.

Other Considerations. In addition to the range and reflectance performance comparisons, the two systems can also be compared in several other respects. Combining Eqs (39) and (47) and taking the bandwidth restriction into account, results in

$$R_{res-PN} = 0.44 R_{res-FM} \tag{59}$$

Eq (59) says that the resolution of the PN system is about 2.3 times better than that of the FM chirp system.

Also, since both modulating signals have the same period, τ_d seconds, their ambiguity intervals are identical. Finally, concerning system implementation, the two systems seem to be about equal. Although components for the FM chirp system may be more readily available, the high sidelobes in the chirp output would cause more of a problem than those of the PN signal.

FM Chirp System and Single Sinusoid System

Range Comparison. The next comparison is between the FM chirp system and the single sinusoid system. The range performance of these two systems can be compared by combining Eqs (23) and (36), resulting in the expression

$$\sigma_{rFM} = 2.4 \frac{f_m}{\Delta f} \sigma_{rs} \tag{60}$$

where σ_{rs} is the standard deviation of the range error for the single sinusoid system. Taking the bandwidth restriction into account by substituting Eq (56) into Eq (60) results in

$$\sigma_{rFM} = 7.2 \frac{f_m}{W} \sigma_{rs} \tag{61}$$

Although the value of f_m is also restricted to an upper limit of W Hz, it would not be practical to use such a high frequency due to ambiguity considerations. Therefore, the value of f_m has been left arbitrary in the above equation.

Eq (61) shows that the relative performance of the two systems depends on the relationship of f_m and W. It can be seen that the FM chirp system will outperform the single sinusoid system if

$$7.2 f_m < W \tag{62}$$

As an example, if f_m is 100 MHz, the detector bandwidth must be greater than 720 MHz for the chirp system to be better. However, if f_m is only 50 MHz, the detector need only have a bandwidth of 360 MHz. In general, a definite statement concerning the required bandwidth cannot be given until it is determined what value f_m should be, i.e., what ambiguity interval can be tolerated in order to meet the operational requirements.

Reflectance Comparison. The reflectance performance of these two systems can be compared by combining Eqs (25) and (37), resulting in

$$\sigma_{\rho FM} = \sigma_{\rho S} \tag{63}$$

Thus, the reflectance performance of the two systems is identical.

Other Considerations. The resolution capabilities of the two systems can be compared by combining Eqs (29) and (39), resulting in

$$R_{res\text{-}FM} = 10.8 \frac{f_m}{W} R_{res\text{-}S} \tag{64}$$

As an example, using the values of f_m = 100 MHz and W = 720 MHz as used in the preceding section, it can be seen that the resolution of the sinusoid system is about 1-1/2 times better than that of the chirp system.

As for the ambiguity comparison, the chirp system is definitely better, since its ambiguity interval is based on the dwell time of the scanner. And, finally, the implementation comparison must lean heavily towards the sinusoid system, since it is a very straightforward and proven method, whereas the chirp technique, although commonly used in radar systems, has never been tried with the laser scanner.

PN On-Off System and Single Sinusoid System

Range Comparison. The final two systems to be compared are the PN on-off system and the single sinusoid system. Combining Eqs (23) and (51) results in the relationship of the standard deviations of the range error given by

$$\sigma_{rPN} = 2.8 f_m t_0 \sigma_{rS} \tag{65}$$

Adding in the bandwidth restriction by substituting Eq (54) into Eq (65)

results in

$$\sigma_{rPN} = 5.6 \frac{f_m}{W} \sigma_{rS} \tag{66}$$

Once again, the relationship between the two systems depends only upon the relationship of f_m and W. Eq (66) shows that the PN on-off system will outperform the single sinusoid system if

$$5.6\ f_m < W \tag{67}$$

Thus, if f_m is 100 MHz, the detector bandwidth must be at least 560 MHz for the PN system to be better. With an f_m of 50 MHz the bandwidth needs to be only greater than 280 MHz.

Reflectance Performance. In order to compare the reflectance performance of the two systems, Eqs (25) and (52) can be combined, resulting in

$$\sigma_{\rho PN} = \frac{1}{\sqrt{2}} \sigma_{\rho S} \tag{68}$$

Thus, the reflectance performance of the PN on-off system is always better than that of the single sinusoid system by a factor of $\sqrt{2}$.

Other Considerations. Another basis for comparison of the two systems is their resolution capabilities. Eqs (29) and (47) can be combined to give

$$R_{res\text{-}PN} = 4.8 \frac{f_m}{W} R_{res\text{-}S} \tag{69}$$

Using the values of 100 MHz for f_m and 560 MHz for W, as used in the preceding section, in Eq (69) result in the fact that the resolution

capability of the PN system is about 1.2 times better than that of the sinusoid system. Comparison of the ambiguity intervals of the two systems also favors the PN system. Since the period of the PN code is τ_d seconds, the ambiguity interval of the PN system is much greater than the largest interval that could be obtained from a useable sinusoid system. And, finally, the implementation comparison favors the sinusoid system, since both the components and the technology required to implement a PN system are much more complex than those required for the sinusoid system.

V. Extension of the Modulation Techniques to a Multiple Source Scanner

In the past several chapters, the modulation techniques described and analyzed were based on a scanner system which contained only one laser source. However, as mentioned previously, when the scanner system is used with high performance aircraft, this single source system may not be adequate. The speed of such an aircraft would require a very fast scan rate in order for the scanner to cover the required ground area in contiguous strips. A fast scan rate results in a very short dwell time. A short dwell time, in turn, results in only a small amount of energy being received from each resolution cell. Since both the range and the reflectance performance of the system are directly proportional to this received energy, a short dwell time may result in a system performance which is unacceptable. The only way to improve the system in such a situation is to reconfigure the scanner itself so that it consists of multiple laser sources instead of just one.

This chapter will take a brief look at two possible methods of setting up just such a multiple source scanner system. Emphasis will be placed not so much on the physical configuration and related problems, but rather on the modulation techniques which could be used in such a system. Since it is only a brief look, further work in this area will be needed in order to determine the feasibility of these two methods.

Multiple Sources in Parallel

Physical Configuration. The first possible configuration for a multiple source scanner is one in which the laser sources sweep out parallel, contiguous strips along the ground (Fig 19, page 65). Assuming that n sources are being used, n parallel strips will be scanned in each

rotation of the scanner. Because of this, the scanner can rotate at a slower speed and still be able to cover the entire area. In fact, it can easily be seen that its rotation speed will be less than the speed required for a single source system by a factor of (1/n). However, because of this slower scan rate, the strips swept out along the ground will not be perpendicular to the flight path of the aircraft, but rather will tend to be more diagonal to it. The difference between the ideal perpendicular strips and the actual strips swept out will increase as the number of sources increases. This may cause a problem with the spatial filtering operation of the scanner and is an area in which further investigation is required.

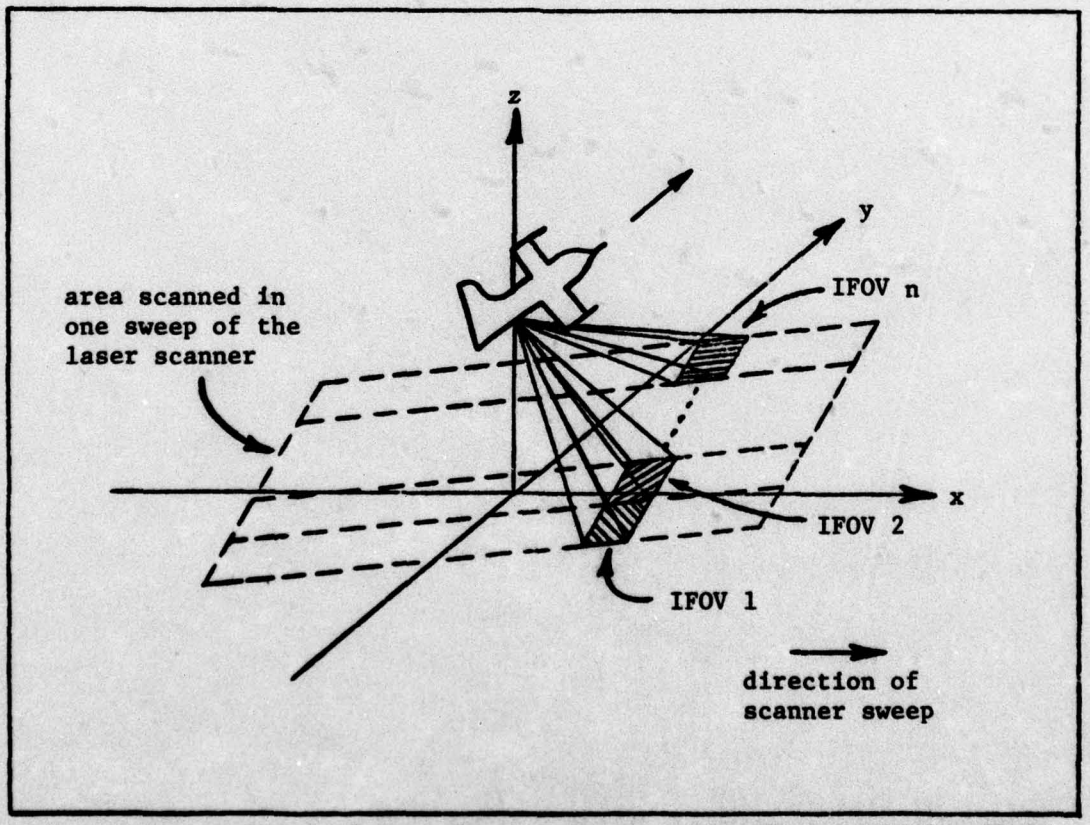

Figure 19. Multiple Source Scanner System using Sources in Parallel

This slower scan speed will also result in a dwell time which is greater than the dwell time of an equivalent single source system by a factor of n. This increased dwell time in turn results in an increase in the received energy per resolution cell and a decrease in the error variance of the system, both also by a factor of n. Thus, paralleling of the laser sources has accomplished its goal by increasing the system performance to an acceptable level. The number of laser sources used will, of course, depend on the relationship between the single-source dwell time and the dwell time required to achieve an acceptable performance.

Possible Modulation Techniques. In order to actually gain the advantage of this multiple source system, the signals transmitted by each laser source must not interfere with each other. That is, the receiver electronics associated with each source must be able to detect only that signal transmitted by its related source and reject the signals from all of the other sources. By choosing modulating frequencies which are separated far enough in frequency, the single sinusoid modulation technique could easily be used with this multiple source system. Filters in each receiver would separate the signals to insure minimum interference, and each receiver would process its own sinusoid exactly as in a single source system. The expressions for the range and the reflectance error variances for each receiver in this system can be found from Eqs (23) and (25), respectively, resulting in

$$\sigma_r^2 = \frac{1}{n} \frac{c^2 N_0}{2\pi^2 f_m^2 P_a^2 R^2 \tau_d} \tag{70}$$

and

$$\sigma_\rho^2 = \frac{1}{n} \frac{4N_0}{P_a^2 R^2 \tau_d} \tag{71}$$

where τ_d is the dwell time of the equivalent single source system. Thus, both the range and the reflectance error variances are decreased by this factor of n. It should be noted that, since the value of f_m is different for each source, the corresponding performance characteristics, including those of resolution and ambiguity, will also vary from source to source. Thus, the overall range performance of the system, as well as its resolution capability, will be limited by the lowest frequency used, whereas the ambiguity interval of the system will be limited by the highest frequency.

Another of the modulation techniques analyzed, the FM chirp technique, does not lend itself to a multiple source system as readily as the sinusoid technique does. The problem with the chirp technique is that it has a very wide bandwidth. In order to avoid interference, the various transmitted signals would have to be separated far enough in frequency so that the unwanted signals could be filtered out in each receiver. However, it was stated earlier that the bandwidth of a chirp signal could easily be near the Gigahertz region in order to obtain the desired performance. Thus, due to bandwidth constraints in the detector, it would be very difficult to use two or more chirp signals in a multiple source system.

The final technique analyzed, the PN on-off system, would also be able to be used in a multiple source system. Each laser source would be modulated with a different PN code, and each receiver would be set up to detect only the particular code word being used by the corresponding

source. The code words can be chosen such that there would be a minimum amount of interference between them. This means that the reception of a code word by a receiver which is matched to a different code word would result in a fairly low, though not constant, sidelobe at the output of the matched filter. This output would still peak only when the code word the receiver is matched to is received (Ref 13: 64-75). Thus, although the matched filter output would not have the constant negative sidelobe associated with a single source system, it nevertheless would still be more than adequate to allow simultaneous operation of n sources with little interference.

The expressions for the range and reflectance error variance for this PN multiple source system can be found from Eqs (51) and (52), respectively, resulting in

$$\sigma_r^2 \cong \frac{1}{n} \frac{\pi c^2 N_0 t_0}{8 P_a^2 R^2 (p+1)} \tag{72}$$

and

$$\sigma_\rho^2 = \frac{1}{n} \frac{2N_0}{P_a^2 R^2 \tau_d} \tag{73}$$

where τ_d and p are the parameters of the equivalent single source system. Thus, the error variances of the system have again been reduced by the factor of n. Also, since all of the code words will have the same chip width, t_0, the resolution of the system will be the same as in the single source scanner. However, since the dwell time has been increased by a factor of n, the ambiguity interval of this system will be n times that of the single source system.

Multiple Sources in Series

Physical Configuration. The second possible configuration for a multiple source scanner is one in which the laser sources sweep along each strip in series (Fig 20, below). Since only one strip is being scanned at a time, the scanner must rotate at the same speed as it would in a single source system. Thus, the dwell time of the scanner, as well as the energy received in each resolution cell, is very small. However, because of the series arrangement, a given receiver will be processing the received energy from a given resolution cell a short period of time after the receiver just ahead of it in the line has processed its received energy from that same resolution cell. Thus, the performance

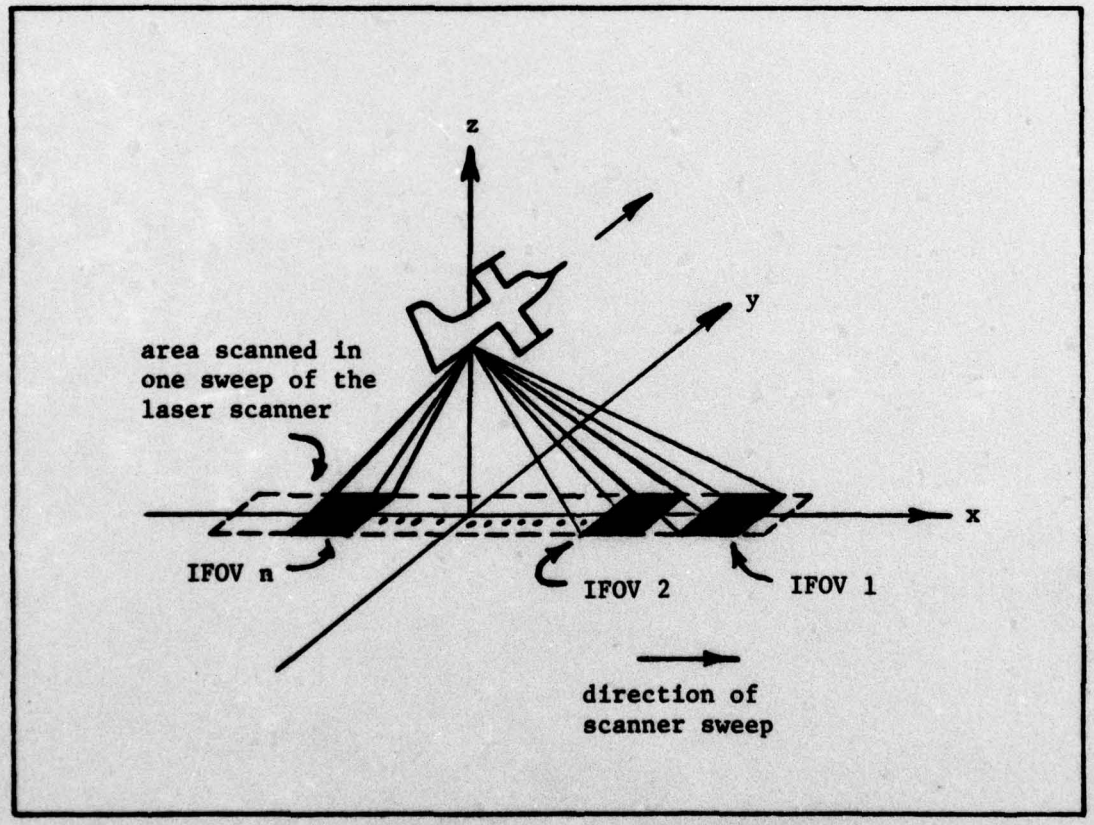

Figure 20. Multiple Source Scanner System using Sources in Series

of this system can be improved by somehow combining all of the energy received by each receiver from a given resolution cell prior to processing it and estimating the slant range and the reflectance of the target. By doing this, the resulting performance of the system will depend on the total energy received from all of the sources rather than just that received from each source individually.

Since only one strip of ground is being scanned at a time, the strips will be nearly perpendicular to the flight path of the aircraft, thus eliminating the spatial filtering problem mentioned in the preceding section. However, since the bandwidth of the spatial information is inversely proportional to the dwell time, the very short dwell time of this configuration will result in a much larger spatial bandwidth than in the parallel system.

In order to achieve the benefits of this multiple source system, the signals used to modulate the lasers not only must not interfere with one another, but also must be capable of being added together such that the energy of the resultant signal is equal to the sum of the energies of all of the individual signals. If this latter condition does not hold, the full potential of the system will not be realized.

Possible Modulation Techniques. In determining which of the various modulation techniques could be used with this system, the FM chirp technique can be immediately eliminated. Since the modulating signals must not interfere with one another, the FM chirp technique is not feasible, as explained in the preceding section. The single sinusoid system is not quite as easy. It is not immediately apparent that a sinusoid system consisting of several different modulating frequencies can be configured such that the received signals could be combined as required.

However, due to a lack of time, not enough effort was expended toward this goal to be able to say that it cannot be done. Thus, this remains an open topic for further study.

The final modulation technique, that of the PN on-off system, could be used with this type of multiple source scanner. Each laser source would be modulated with a different PN code word, as explained previously. Thus, each receiver would be matched to a particular code word and would process the received signal through the delay line-summer network as in a single source system (Fig 21, page 72). However, instead of routing the output of this network into a matched filter, it would be sent into another delay line. In this delay line, the time delay between taps would be equal to the time difference between two adjacent laser sources scanning the same resolution cell. Thus, at the output of the delay line, the signals received by each receiver from the same resolution cell will have added together, resulting in a single pulse of width t_0 seconds and amplitude n times the amplitude of the individual pulses, where n is the number of sources being used in the system. This single pulse would then be sent through a matched filter, and the output would be proportional to the total energy received from that resolution cell, rather than just the energy received by one of the receivers.

The expressions for the range and reflectance error variances for this system can again be found from Eqs (51) and (52), respectively, resulting in the same expressions found for the parallel source system:

$$\sigma_r^2 \approx \frac{1}{n} \frac{\pi c^2 N_0 t_0}{8 P_a^2 R^2 (p+1)} \tag{72}$$

and

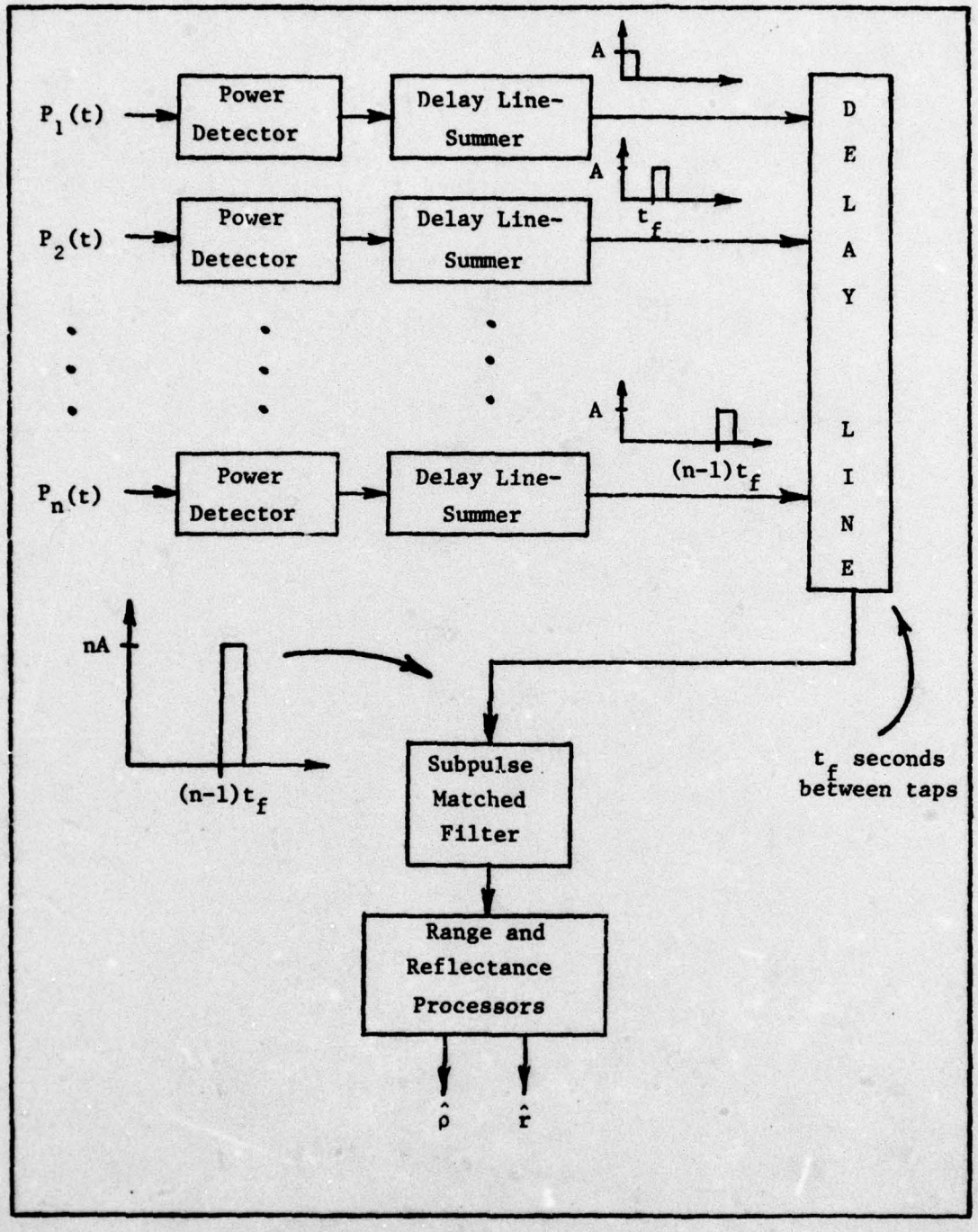

Figure 21. Receiver Configuration for a Series Multiple Source System using PN Coding

$$\sigma_\rho^2 = \frac{1}{n} \frac{2N_0}{P_a^2 R^2 \tau_d} \tag{73}$$

Thus, the performance of this multiple source system has been improved by the same factor of n as in the parallel source system, only this time the improvement is due to the summing of the received signals rather than to the lengthening of the dwell time. Also, for this system both the resolution and the ambiguity interval are the same as in a single source scanner.

VI. Conclusions and Recommendations

Now that all of the analyses and comparisons have been completed, it is time to look at the results and to try and draw some conclusions from them. This chapter will attempt to do just that, by first presenting some general conclusions and then by making several recommendations for future work in this area.

Conclusions

The main purpose of this study was to investigate various methods of modulating a peak-power limited laser and to analyze the performance characteristics of each technique. This objective was accomplished by analyzing four different techniques which appeared to be the most promising possibilities. In addition, these four techniques were compared to one another on the basis of their computed performance. Although the next logical step is to choose the best technique based on these comparisons, it cannot be stated that one technique is always superior to the others unless specific ground rules are first laid down concerning the acceptable level of ambiguity and the available detector bandwidth.

Even though such a definite conclusion cannot be made, several general conclusions can be reached from this study. To begin with, it appears that the single sinusoid system, the FM chirp system, and the PN on-off system are all feasible for use with a single source scanner. However, problems concerning the actual modulation of the laser would have to be investigated before either the FM chirp or the PN systems could be implemented.

In addition, if the main goal of the system is simplicity and cost-effectiveness and if the short ambiguity interval is not a problem, then

the single sinusoid system appears to be the preferred technique. However, if the ambiguity interval is indeed a major consideration, then the PN system is the system to use. Although the chirp system is also feasible in this case, it would require a greater detector bandwidth for the same performance and thus would not have much of an advantage over the PN system. Since the PN system, as well as the chirp system, trades bandwidth for performance, using it in place of the single sinusoid system places a much more stringent requirement on the bandwidth of all of the system components, especially on the power detector. However, since its ambiguity interval is dependent only on the dwell time of the scanner, and since its performance improves as its bandwidth increases, the PN system is definitely the one to use if the required bandwidth is available.

These same conclusions can be easily extended to the case of a multiple source scanner. Although both the sinusoid system and the PN system are feasible with a multiple source scanner, the one to use will really depend on the system requirements; namely, what kind of ambiguity can be tolerated, how large a bandwidth is available, and how is the multiple source scanner configured. However, once again, if the bandwidth is available and if the additional equipment complexity is justified, the PN system appears to be the system to use.

Recommendations

Based on the conclusions stated above, the first recommendation for further work in this area is for a detailed study to examine the problems involved in the implementation of a PN coded laser scanner system. This study was designed to be mainly a theoretical study and, as such, has looked only briefly at the practical problems involved in such an

implementation. As a part of this new study, efforts should be made to determine at how high a rate a semiconductor laser can be modulated, since this is really the key issue in using a PN system.

In addition to the PN study, there are two portions of this study which should be expanded. The first expansion is to determine the effect of the spatial filtering operation of the scanner on the wideband transmitted signal in both the FM chirp and the PN systems. The second one is to expand that portion which deals with a multiple source scanner. In particular, the two configurations described, as well as any other promising configurations, should be examined in more detail in order to analyze the problems that would be encountered in each system and to determine which one would be the best one to use.

The final recommendation for further work is to continue the main theme of this study by analyzing additional methods of modulating the laser. Although the four techniques analyzed in this study appear to be the most promising techniques, they are not the only possibilities. Additional techniques exist, especially in the area of coded waveforms and nonlinear FM waveforms, and should be analyzed and compared to the techniques described in this study.

Bibliography

1. Perkin-Elmer Corporation. Gallium Arsenide (GaAs) Diode Laser, RF Experiment Results. Report No. 13170. Norwalk, Connecticut: Perkin-Elmer Corporation, October 1976.

2. Cook, Charles E. and Marvin Bernfeld. Radar Signals: An Introduction to Theory and Application. New York: Academic Press, Inc., 1967.

3. Van Trees, Harry L. Detection, Estimation, and Modulation Theory, Part III: Radar-Sonar Signal Processing and Gaussian Signals in Noise. New York: John Wiley & Sons, Inc., 1971.

4. Wozencraft, John M. and Irwin Mark Jacobs. Principles of Communication Engineering. New York: John Wiley & Sons, Inc., 1965.

5. Lindsey, William C. and Marvin K. Simon. Telecommunication Systems Engineering. Englewood Cliffs, New Jersey: Prentice-Hall, Inc., 1973.

6. Van Trees, Harry L. Detection, Estimation, and Modulation Theory, Part II: Nonlinear Modulation Theory. New York: John Wiley & Sons, Inc., 1971.

7. Van Trees, Harry L. Detection, Estimation, and Modulation Theory, Part I: Detection, Estimation, and Linear Modulation Theory. New York: John Wiley & Sons, Inc., 1968.

8. Rihaczek, August W. Principles of High-Resolution Radar. New York: McGraw-Hill Book Company, 1969.

9. Farnett, Edward C., et al. "Pulse-Compression Radar" in Radar Handbook, edited by Merrill I. Skolnik. New York: McGraw-Hill Book Company, 1970.

10. Weglein, Rolf D. "SAW Chirp Filter Performance Above 1 GHz." Proceedings of the IEEE, 64: 695-698 (May 1976).

11. Morgan, D. P. and J. P. Sutherland. "Generation of Pseudonoise Sequences using Surface Acoustic Waves." IEEE Transactions on Sonics and Ultrasonics, SU-20: 224 (April 1973).

12. Bell, DeLamar T., et al. "Application of Acoustic Surface-Wave Technology to Spread-Spectrum Communications." IEEE Transactions on Sonics and Ultrasonics, SU-20: 181-189 (April 1973).

13. Dixon, R. C. Spread Spectrum Systems. New York: John Wiley & Sons, Inc., 1976.

14. Lathi, B. P. Communications Systems. New York: John Wiley & Sons, Inc., 1968.

15. Easterling, Mahlon F. "Modulation by Pseudo-Random Sequences" in Digital Communications with Space Applications edited by Solomon W. Golomb. Englewood Cliffs, New Jersey: Prentice-Hall, Inc., 1964.

16. Gradshteyn, I. S. and I. M. Ryzhik. Tables of Integrals, Series, and Products. New York: Academic Press, 1965.

Appendix A

Leading-Edge Derivation of the Range-Error Variance for an FM Chirp System

In Chapter II, it was stated that in order to use the Cramer-Rao lower bound for the range error variance, the noise must be Gaussian. It was also stated that the range error variance could be derived using a leading-edge analysis which does not require the assumption of Gaussian noise. This appendix will present a description of this leading-edge analysis for the FM chirp waveform, and will compare the variance obtained with that obtained using the Cramer-Rao expression.

The output of the compression filter in the FM chirp receiver has the form of a sin x/x pulse (Fig 22, below). The width of the mainlobe of this pulse is $2/\Delta f$, where Δf is the frequency deviation of the chirp pulse. In order to generate a range estimate, this output is sent through a detector which marks the instant of time that the output exceeds a predetermined threshold. The time delay thus measured is then easily converted to the desired slant range estimate.

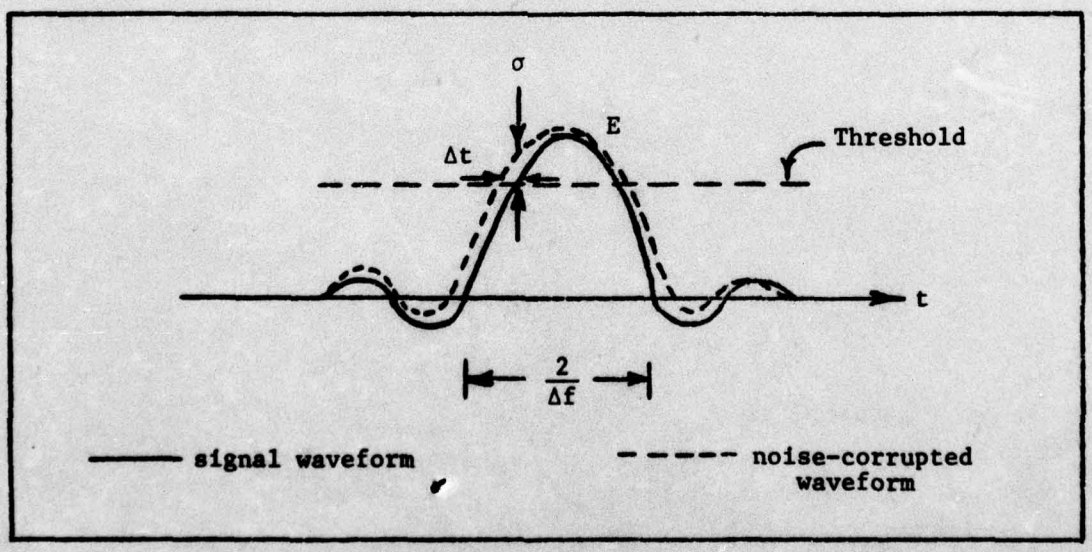

Figure 22. Output Waveform of the Compression Filter in an FM Chirp System

The effect of additive noise in the output signal is to cause the output to exceed the threshold either sooner than it should or later. Thus, the time measurement of the detector is in error by some increment of time, Δt seconds. The magnitude of this time error is dependent both on the noise power at the filter output and on the slope of the noise corrupted waveform in the vicinity of the threshold. Assuming that the noise at the filter output is slowly varying in relation to the signal, and that the signal-to-noise ratio is much greater than one, the slope of the noise-corrupted output is approximately the same as that of the uncorrupted signal output. Therefore, the first item needed for this analysis is an expression for the slope of the signal waveform in the vicinity of the threshold. This slope can be adequately approximated by the slope of a straight line from the edge of the mainlobe to its half-power point. After a little algebra, this slope is calculated to be

$$S_u = 1.3\,E\Delta f \tag{74}$$

where E, the energy of the signal at the input to the filter, is the peak value of the filter output.

The differential change in the waveform caused by the noise can now be equated to Eq (74), resulting in

$$\frac{\sigma}{\Delta t} = 1.3\,E\Delta f \tag{75}$$

where σ and Δt are the root-mean-square (rms) values of the noise power and the time error, respectively. Rearranging Eq (75) leads to an expression for the rms time error:

$$\Delta t = \frac{\sigma}{1.3\,E\Delta f} \tag{76}$$

Eq (76) can be changed to an rms range error by using the relation

$$\Delta r = \frac{c}{2}\,\Delta t \tag{77}$$

which results in

$$\Delta r = \frac{c\sigma}{2.6\,E\Delta f} \tag{78}$$

Assuming that the noise at the input to the filter is white, with a double-sided power spectral density of $N_0/2$ watts/Hz, the variance of the noise at the output of the filter can be found by integrating the noise power spectral density at the output,

$$\sigma^2 = \frac{N_0}{2} \int_{-\infty}^{\infty} |U(f)|^2 df \tag{79}$$

where U(f) is the frequency response of the filter. However, since the filter is matched to the FM chirp pulse, the integral in Eq (79) is just the energy in the signal. Thus,

$$\sigma^2 = \frac{N_0 E}{2} \tag{80}$$

and

$$\Delta r = \frac{c}{2.6\,E\Delta f} \sqrt{\frac{N_0 E}{2}} \tag{81}$$

Simplifying Eq (81) and substituting in the value of E given by Eq (34) results in

$$\Delta r = \frac{c\sqrt{N_0}}{1.3\,\Delta f P_a R\sqrt{\tau_d}} \tag{82}$$

Thus, the variance of the range error is just the square of Eq (82):

$$\sigma_r^2 = \frac{c^2 N_0}{1.69\,\Delta f^2 P_a^2 R^2 \tau_d} \tag{83}$$

Comparison of the error variance derived above and the one derived by means of the Cramer-Rao bound can be easily accomplished by combining Eqs (36) and (83). The result is

$$\sigma_{rLE}^2 \simeq 1.9\,\sigma_{rCR}^2 \tag{84}$$

where σ_{rLE}^2 and σ_{rCR}^2 are the error variances obtained by the leading-edge analysis and the Cramer-Rao method, respectively. As can be seen, the leading-edge variance is higher than the Cramer-Rao variance by a factor of approximately 1.9. In terms of standard deviations, it is higher by a factor of about 1.4. Thus, although the assumption of Gaussian noise results in a lower value for the error variance, elimination of this assumption does not significantly alter the value of the variance.

Appendix B

Derivation of the Mean-Squared Bandwidth for a Pseudonoise-Coded System

The purpose of this appendix is to derive the expression for the mean-squared bandwidth of a pseudonoise (PN) coded binary waveform (Fig 13, page 41). From Eq (3), the expression for this bandwidth is

$$\beta^2 = \frac{4\pi^2 \int_{-\infty}^{\infty} f^2 |U(f)|^2 df}{\int_{-\infty}^{\infty} |U(f)|^2 df} \tag{3}$$

where $|U(f)|$ is the magnitude of the frequency spectrum of the binary waveform. Eq (3) can be written in terms of radian frequencies as

$$\beta^2 = \frac{\int_{-\infty}^{\infty} \omega^2 |U(\omega)|^2 d\omega}{\int_{-\infty}^{\infty} |U(\omega)|^2 d\omega} \tag{85}$$

where ω is the frequency in radians/sec.

Since u(t) is a periodic function, the power density spectrum of u(t), denoted by $S_u(\omega)$, is related to the Fourier transform of the signal, $U(\omega)$, by the equation (Ref 14: 137)

$$S_u(\omega) = \frac{1}{2\pi} |U(\omega)|^2 \tag{86}$$

Eq (85) can now be written in terms of the power density spectrum as

$$\beta^2 = \frac{\int_{-\infty}^{\infty} \omega^2 S_u(\omega) d\omega}{\int_{-\infty}^{\infty} S_u(\omega) d\omega} \tag{87}$$

However, one of the characteristics of a power density spectrum is that

$$\frac{1}{2\pi}\int_{-\infty}^{\infty} S_u(\omega)d\omega = P \tag{88}$$

where P is the average power in the signal (Ref 14: 132). Therefore, Eq (87) can be written as

$$\beta^2 = \frac{\int_{-\infty}^{\infty}\omega^2 S_u(\omega)d\omega}{2\pi P} \tag{89}$$

The value of the average power, P, can be found from the binary waveform, u(t). Since this waveform alternates between ±1 and has a period of pt_0 seconds, its average power is

$$P = \frac{\int_0^{pt_0} u^2(t)dt}{pt_0} = 1 \tag{90}$$

Thus, Eq (89) can be further simplified to

$$\beta^2 = \frac{1}{2\pi}\int_{-\infty}^{\infty}\omega^2 S_u(\omega)d\omega \tag{91}$$

The next step in the derivation is to use the expression for the power spectral density of a PN waveform which is given by the equation (Ref 15: 76)

$$S_u(\omega) = S_{PN}(\omega) = \left(\frac{p+1}{p^2}\right)\left(\frac{\sin\frac{\omega t_0}{2}}{\frac{\omega t_0}{2}}\right)^2 \sum_{\substack{n=-\infty \\ n\neq 0}}^{\infty} \delta\left(\omega - \frac{2\pi n}{pt_0}\right) + \frac{1}{p^2}\delta(\omega) \tag{92}$$

where $\delta(\omega)$ is the Dirac delta function, or impulse function (Ref 14: 46-49). Since the waveform is periodic, this spectrum consists of discrete

spectral lines which are separated by $2\pi/pt_0$ radians/sec (Fig 23, page 86). Substituting Eq (92) in Eq (91) results in

$$\beta^2 = \left(\frac{p+1}{2\pi p^2}\right) \int_{-\infty}^{\infty} (\omega^2) \left(\frac{\sin \frac{\omega t_0}{2}}{\frac{\omega t_0}{2}} \right)^2 \sum_{\substack{n=-\infty \\ n\neq 0}}^{\infty} \delta\left(\omega - \frac{2\pi n}{pt_0}\right) d\omega + \frac{1}{2\pi p^2} \int_{-\infty}^{\infty} \omega^2 \delta(\omega) d\omega \quad (93)$$

The last integral in Eq (93) is zero due to the sifting property of the delta function (Ref 14: 51). Also, the infinite sum in the first integral can be simplified by noting that the envelope of the spectrum is a $(\sin x/x)^2$ function. Assuming that the significant portion of this envelope extends out to the second zero crossing on each side of the spectrum, the limits on the infinite sum can be correspondingly reduced, resulting in

$$\beta^2 = \left(\frac{p+1}{2\pi p^2}\right) \int_{-\infty}^{\infty} (\omega^2) \left(\frac{\sin \frac{\omega t_0}{2}}{\frac{\omega t_0}{2}} \right)^2 \sum_{\substack{n=-2p \\ n\neq 0}}^{2p} \delta\left(\omega - \frac{2\pi n}{pt_0}\right) d\omega \quad (94)$$

Interchanging the order of integration and summation, and integrating each term in the sum by use of the sifting property of the delta function results in

$$\beta^2 = \left(\frac{p+1}{2\pi p^2}\right) \sum_{\substack{n=-2p \\ n\neq 0}}^{2p} \left(\frac{4\pi^2 n^2}{p^2 t_0^2}\right) \left(\frac{\sin \frac{\pi n}{p}}{\frac{\pi n}{p}} \right)^2 \quad (95)$$

Further algebraic reduction reduces Eq (95) to

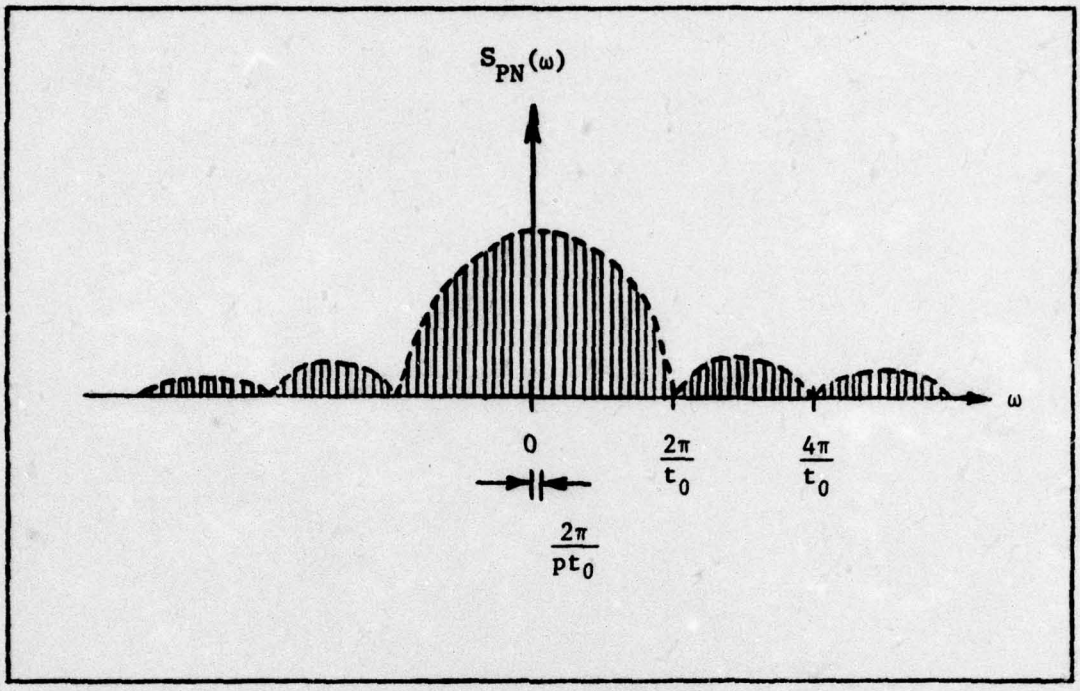

Figure 23. Power Spectral Density of a PN Waveform (from Ref 15: 77)

$$\beta^2 = \left(\frac{p+1}{2\pi p^2}\right)\left(\frac{4}{t_0^2}\right)\sum_{\substack{n=-2p \\ n\neq 0}}^{2p} \sin^2\left(\frac{\pi n}{p}\right) \tag{96}$$

Symmetry of the $\sin^2(x)$ function reduces Eq (96) to

$$\beta^2 = \frac{4(p+1)}{\pi p^2 t_0^2}\sum_{n=1}^{2p} \sin^2\left(\frac{\pi n}{p}\right) \tag{97}$$

Fortunately, the sum in Eq (97) has been tabulated (Ref 16: 30). Using this tabulation, Eq (97) can be reduced to the final expression for the mean-squared bandwidth:

$$\beta^2 = \frac{4(p+1)}{\pi p t_0^2} \tag{98}$$

Thus, it can be seen that β^2 is dependent on both the length of the code,

p, and the chip width, t_0. However, since p and (p+1) pretty much cancel each other out, the only significant variable in the equation is t_0. As the chip width of the code is decreased, the significant portion of the frequency spectrum of the code is increased, thus also increasing the value of the mean-squared bandwidth.

Appendix C

Leading-Edge Derivation of the Range-Error Variance for a Pseudonoise Coded System

The purpose of this appendix is to derive an expression for the range error variance of a pseudonoise (PN) coded system, and to compare this variance with the one obtained by using the Cramer-Rao lower bound. The derivation will follow the same general line of reasoning used in the derivation of the error variance for the FM chirp system described in Appendix A.

The output of the subpulse matched filter has a triangular-shaped envelope in the absence of noise (Fig 24, page 89). Since the output has a total width of $2t_0$ seconds and a peak value equivalent to the energy, E, in the received signal, the slope of this output signal is found to be

$$S_u = \frac{E}{t_0} \tag{99}$$

The differential change in the waveform caused by the noise can be equated to Eq (99), resulting in

$$\frac{\sigma}{\Delta t} = \frac{E}{t_0} \tag{100}$$

where σ and Δt are again the root-mean-square (rms) values of the noise and the time error, respectively. Rearranging Eq (100) results in

$$\Delta t = \frac{\sigma t_0}{E} \tag{101}$$

Using the value for σ^2 given by Eq (80),

AD-A035 291 AIR FORCE INST OF TECH WRIGHT-PATTERSON AFB OHIO SCH--ETC F/G 20/5
AN ANALYSIS OF MODULATION TECHNIQUES FOR THE SIMULTANEOUS MEASU--ETC(U)
DEC 76 R C CHAPURAN

UNCLASSIFIED GE/EE/76-18 NL

2 OF 2
AD A035291

END
DATE FILMED
3-77

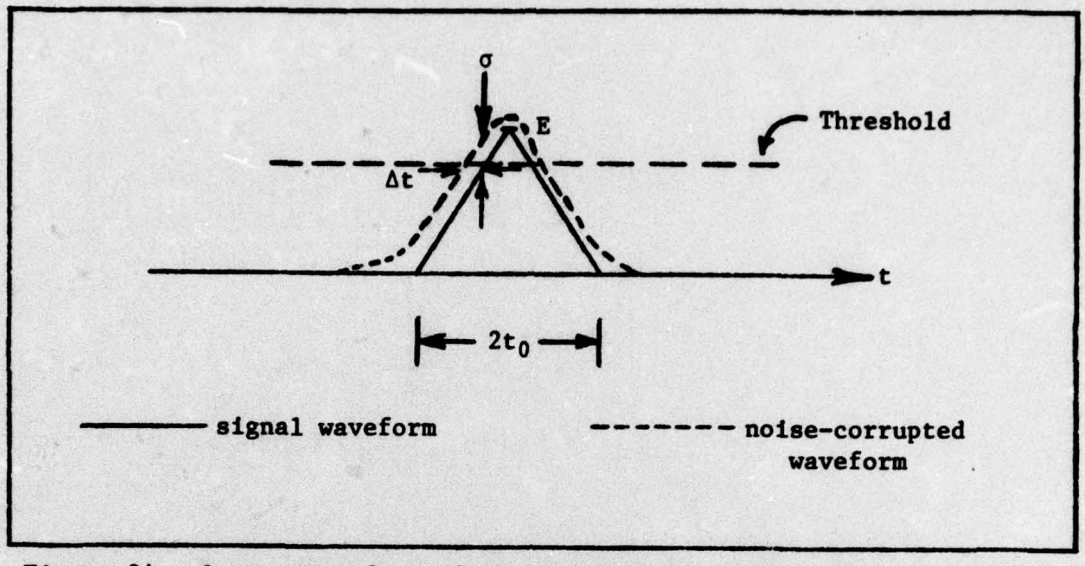

Figure 24. Output Waveform of the Matched Filter in a PN Coded System

$$\sigma^2 = \frac{N_0 E}{2} \tag{80}$$

results in

$$\Delta t = \frac{t_0 \sqrt{N_0}}{\sqrt{2E}} \tag{102}$$

Substituting Eq (102) into the relation between time error and range error given by Eq (79) results in

$$\Delta r = \frac{c t_0 \sqrt{N_0}}{2\sqrt{2E}} \tag{103}$$

Substituting in the value of E given by Eq (42) and squaring the result gives the final expression for the range variance:

$$\sigma_r^2 = \frac{c^2 t_0^2 N_0}{P_a^2 R^2 \tau_d} \tag{104}$$

The final step is to compare the error variance derived above with the variance derived using the Cramer-Rao bound. This latter variance, given by Eq (44), can be combined with Eq (104), resulting in

$$\sigma_{rLE}^2 \simeq 1.3\,\sigma_{rCR}^2 \tag{105}$$

where σ_{rLE}^2 and σ_{rCR}^2 are the error variances obtained by the leading-edge and the Cramer-Rao methods, respectively. As can be seen, the leading-edge variance is higher than the Cramer-Rao variance by a factor of approximately 1.3. In terms of standard deviations, the difference is only a factor of about 1.1. Thus, for the case of the PN coded system, eliminating the assumption of Gaussian noise makes very little difference in the resulting range error variance.

VITA

Robert Charles Chapuran was born on 29 February 1948 in Omaha, Nebraska. He graduated from high school in Omaha in 1966 and attended Iowa State University from which he received the degree of Bachelor of Science, Electrical Engineering, in November 1970. Upon graduation, he received a commission in the USAF through the AFROTC program. His first assignment was to attend the Communications-Electronics Engineer Course at the Keesler Technical Training Center, Keesler AFB, Mississippi. Upon completion of the course in July 1971, he was assigned to Headquarters, Southern Communications Area, Oklahoma City Air Force Station, Oklahoma, where he served as a Base Wire Engineer. In June 1974, he was sent to Osan AB, Republic of Korea, where he served as the Telecommunications Systems Staff Officer in the 2146th Communications Group (AFCS) until entering the School of Engineering, Air Force Institute of Technology, in May 1975.

Permanent address: 1706 S. 11 St
Omaha, Nebraska 68108

UNCLASSIFIED
SECURITY CLASSIFICATION OF THIS PAGE (When Data Entered)

REPORT DOCUMENTATION PAGE		READ INSTRUCTIONS BEFORE COMPLETING FORM
1. REPORT NUMBER GE/EE/76-18	2. GOVT ACCESSION NO.	3. RECIPIENT'S CATALOG NUMBER
4. TITLE (and Subtitle) AN ANALYSIS OF MODULATION TECHNIQUES FOR THE SIMULTANEOUS MEASUREMENT OF RANGE AND REFLECTANCE INFORMATION BY AN AIRBORNE LASER SCANNER		5. TYPE OF REPORT & PERIOD COVERED MS Thesis 6. PERFORMING ORG. REPORT NUMBER
7. AUTHOR(s) Robert C. Chapuran Captain, USAF		8. CONTRACT OR GRANT NUMBER(s)
9. PERFORMING ORGANIZATION NAME AND ADDRESS Air Force Institute of Technology (AFIT-EN) Wright-Patterson AFB, Ohio 45433		10. PROGRAM ELEMENT, PROJECT, TASK AREA & WORK UNIT NUMBERS
11. CONTROLLING OFFICE NAME AND ADDRESS Electro-Optics and Reconnaissance Branch (AFAL-RWI) Air Force Avionics Laboratory Wright-Patterson AFB, Ohio 45433		12. REPORT DATE DECEMBER, 1976 13. NUMBER OF PAGES 100
14. MONITORING AGENCY NAME & ADDRESS(if different from Controlling Office)		15. SECURITY CLASS. (of this report) Unclassified 15a. DECLASSIFICATION/DOWNGRADING SCHEDULE

16. DISTRIBUTION STATEMENT (of this Report)

Approved for public release; distribution unlimited.

17. DISTRIBUTION STATEMENT (of the abstract entered in Block 20, if different from Report)

18. SUPPLEMENTARY NOTES

Approved for public release; IAW AFR 190-17

JERRAL F. GUESS, Captain, USAF
Director of Information

19. KEY WORDS (Continue on reverse side if necessary and identify by block number)

Target Cueing
Target Acquisition
Terrain Mapping
Laser Line Scanner
Laser Rangefinders

20. ABSTRACT (Continue on reverse side if necessary and identify by block number)

The performance of an airborne laser terrain mapper, which measures both slant range and reflectance, depends on the method used to modulate the output power of the laser. This study analyzes four possible modulation techniques for a direct-detection scanner which utilizes a semiconductor laser.

The first technique is sinusoidal modulation of the laser output. Range performance is found to improve as the frequency of the modulating sinusoid is increased. The second technique modulates the laser output with a subcarrier

DD FORM 1 JAN 73 1473 EDITION OF 1 NOV 65 IS OBSOLETE

UNCLASSIFIED
SECURITY CLASSIFICATION OF THIS PAGE (When Data Entered)

which is a periodic FM chirp pulse. Range performance improves as the frequency deviation of the chirp is increased. However, this also increases the required detector bandwidth. The third technique modulates the laser with a subcarrier which is phase-modulated by a periodic pseudonoise (PN) code. Although range performance improves as the chip width of the code is decreased, this again requires increased bandwidth. The final technique modulates the laser output directly with a PN code, the output being either on or off. Range performance again depends on the chip width, and improved performance again requires larger bandwidths. Comparisons of these techniques shows that the PN on-off method is preferred if sufficient bandwidth is available. Two configurations for a multiple-source scanner are also proposed. It is shown that both the sinusoid and the PN on-off methods are compatible with such a scanner.